Microalgae-derived HEFA Jet Fuel: Environmental and Economic Impacts of Scaled/Integrated Growth Facilities and Global Production Potential

by

Jacob L. Ames

B.S. Mechanical Engineering
Saint Martin's University, 2012

Submitted to the Department of Aeronautics and Astronautics in Partial Fulfillment of the Requirements for the Degree of

Master of Science in Aeronautics and Astronautics

at the

MASSACHUSETTS INSTITUTE OF TECHNOLOGY

FEBRUARY 2015

Signature redacted

Signature of Author: _____

Department of Aeronautics and Astronautics
January 29, 2015

Signature redacted

Certified by: _____

Steven R.H. Barrett
Associate Professor of Aeronautics and Astronautics
Thesis Supervisor

Signature redacted

Accepted by: _____

Paulo C. Lozano
Associate Professor of Aeronautics and Astronautics
Chair, Graduate Program Committee

[Page Intentionally Left Blank]

Microalgae-derived HEFA Jet Fuel: Environmental and Economic Impacts of Scaled/Integrated Growth Facilities and Global Production Potential

by

Jacob L. Ames

Submitted to the Department of Aeronautics and Astronautics on
January 29, 2015 in Partial Fulfillment of the Requirements for the Degree of
Master of Science in Aeronautics and Astronautics

Abstract

Biofuels have the potential to mitigate the environmental impact of aviation and offer increased energy security through the displacement of conventional jet fuel. This study investigates strategies designed to reduce the production cost and lifecycle greenhouse gas (GHG) emissions of microalgae-derived HEFA jet fuel. Additionally, the global production potential of HEFA-J is quantified in order to assess the efficacy of microalgae as an energy crop.

Impacts from the integration/scaling of microalgae cultivation were quantified by calculating avoided costs and GHG emissions from inputs displaced as a result of integration/scaling. Avoided costs and emissions associated with each impacted input were calculated in units of $\$/gal_{HEFA-J}$ and gCO_2e/MJ_{HEFA-J}, respectively. Results were summed to produce total impact values and resulting production cost/lifecycle emissions values of HEFA-J for each strategy investigated.

Baseline results indicate that integration with wastewater treatment (WWT) facilities may reduce production cost and lifecycle GHG emissions of HEFA-J by 29.2% and >100%, respectively, in open pond systems. Integration with aquaculture processes may reduce production cost by 10.4% in open ponds. Scaling microalgae cultivation from 137 to 2192 barrels per day (BPD) results in a 22.7% reduction in production cost and a 32.0% reduction in lifecycle GHG emissions in open pond systems. Combining scaling and WWT integration methods in open ponds yields a 52.0% reduction in production cost and >100% lifecycle GHG emissions reduction.

Global production potential of microalgae-derived HEFA-J is quantified through the summation of annual energy yields of cells at a 5 arc minute resolution. Results are constrained by geographically variable biological growth factors in addition to water/CO_2 transportation constraints, land availability and slope, and industrial CO_2 availability. Maximum jet and maximum distillate product slates were applied to total energy potential results to quantify global production potential of HEFA-J. Baseline results indicate that 27.5 EJ_{HEFA-J}/yr may be produced, or approximately 3 times the annual global aviation energy demand.

Thesis Supervisor: Steven R. H. Barrett
Title: Associate Professor of Aeronautics and Astronautics

[Page Intentionally Left Blank]

Acknowledgements

I would first like to offer my sincere thanks and appreciation to both of my thesis advisors, Professor Steven Barrett and Dr. Robert Malina. In addition to making this work possible, their advice and guidance throughout my educational career at MIT have encouraged me to explore opportunities outside my academic curriculum and gain valuable professional and life experience. I would also like to thank the Federal Aviation Administration for the financial support of this work, and especially recognize Dr. James Hileman of the FAA for regularly offering his time and expert advice. Additionally, I extend my gratitude to Mr. Nicholas Carter, whose work has served as the framework for a large portion of my own.

I have been fortunate enough to spend my last two years in the Laboratory for Aviation and the Environment with a number of exceptional individuals who have assisted me in my work, offered excellent advice, and kept me sane in times of stress with good humor. In particular, I'd like to thank Mr. Matthew Pearlson for his invaluable mentorship and organization of laboratory events, and my good friend and colleague Mr. Parthsarathi Trivedi for his support in both my work at MIT and my life as a student.

I'd like to express my sincerest appreciation for all the love and encouragement I've received from my family over the last two years and throughout my life, without which none of this would have been achievable. To my parents, Gary and Carolyn, my grandmother Theresa, my best man and brother David, my aunts, uncles, cousins, closest friends, and my grandfather Leroy, who is undoubtedly smiling above – I thank you, and I love you.

Finally, to my incredible wife Sarah, who has been with me through some of the toughest times in my life and supported me to no end, who has picked me up when I couldn't lift myself, who has worked tirelessly to make this beautiful life possible, and who knew that I could when I thought I couldn't – I thank you, and I will love you always. We made it.

[Page Intentionally Left Blank]

Table of Contents

[Page Intentionally Left Blank]

List of Figures

List of Tables

[Page Intentionally Left Blank]

1 - Introduction

Aviation currently contributes around 2% of global anthropogenic CO_2 emissions and 12% of CO_2 emissions from all transportation sources (ICAO, 2010), and projections indicate that, without mitigation, greenhouse gas (GHG) emissions from aviation may increase by a factor of 2.8 – 3.9 by 2040 (ICAO, 2013). In the United States, the annual growth rate of the aviation industry is approximately 5% and, without intervention, aviation GHG emissions in the U.S. have been forecast to increase by a factor of 4 by 2050 (McCollum & Yang, 2009).

Microalgae may have the potential to mitigate the GHG footprint of aviation by being used as an energy feedstock for the production of "drop-in" biofuels with lower lifecycle GHG emissions than conventional jet fuel. Drop-in fuels are chemically similar to conventional jet fuels, such that they can be used in the existing aircraft fleet and fuel distribution infrastructure (Stratton et al., 2010). Drop-in aviation biofuels can be produced from a wide variety of terrestrial crops. However, constraints such as low areal energy yield, required soil fertility, and extensive land requirements, among others, limit their potential for energy production (Carter, 2012).

Microalgae has received attention from the bioenergy industry for a number of reasons. In particular, projections for microalgae areal energy yields fall between 15,000-25,000 L/ha/yr, exceeding the areal yield of competing photoautotrophic energy crops by a factor of at least 6 (Carter, 2012). Other estimates suggest that yields upwards of 30,000 L/ha/yr may be achieved (Hu et al., 2008). Microalgae can also be cultivated in areas otherwise unsuitable for plant growth, such as the southwestern United States, and can utilize carbon dioxide present in flue gas of coal-fired and natural gas power plants (Menetrez, 2012). Finally, many species are capable of growing in brackish or seawater, reducing the potential for conflict between bioenergy and agricultural industries (Carter, 2012; Florentinus et al, 2008).

The economic viability and lifecycle GHG emissions of microalgae-derived jet fuel have been the subject of previous analyses. In a study by Carter (2012), an analysis was performed on several methods of algae-derived HEFA jet fuel production indicating that, as a baseline, microalgae-derived jet fuel may be produced at $\$9.86/gal_{HEFA\text{-}J}$ in an open raceway pond system using wet extraction, with associated lifecycle GHG emissions of 31.3 $gCO_2e/MJ_{HEFA\text{-}J}$. These results are based on a pilot scale facility producing 137 barrels per day (BPD) of HEFA jet fuel in the southwestern United States, supplemented by carbon dioxide present in flue gas diverted from industrial coal power plants. In comparison, conventional jet fuel was available at $2.88 per gallon as of May 2014, and may double in price by 2050 (Eggers, 2013). The lifecycle GHG emissions of conventional jet fuel are estimated to be 87.5 gCO_2e/MJ (Stratton et al., 2010).

Integrating microalgae cultivation sites with facilities producing nutrient-rich effluent may be an option for reducing both production cost and lifecycle emissions of microalgae-derived fuel. Additionally, scaling the microalgae cultivation facility to commercial yield may lead to reductions in staffing/capital costs and input requirements, reducing production costs and lifecycle GHG emissions (Carter, 2012).

Jet fuel derived from microalgae has shown potential to reduce aviation-related GHG emissions, but it is necessary to quantify the long-term potential for microalgae-derived jet fuel production on a global scale. In 2012, the aviation industry consumed 72 billion gallons or just over 9 EJ of jet fuel, and consumption is projected to continually increase over the coming years (International Air Transportation Association, 2013). Quantifying the annual global energy potential of microalgae may assist in determining its efficacy to displace a portion of conventional jet fuel demand.

There is existing literature on the sustainability of alternative jet fuel production, specifically using microalgae as an energy feedstock. Stratton et al. (2010) carries out an analysis to assess the lifecycle GHG emissions of a range of fuel production pathways, and Carter (2012) subsequently focuses in-depth on microalgae-derived jet fuel. In particular, Carter (2012) assesses the economic and environmental viability of HEFA jet fuel production using four different cultivation technologies in a pilot scale facility. Menetrez (2012) and Hu et al. (2008) have performed similar economic and environmental feasibility studies. Olguin (2012) and Woertz et al. (2009) assess the prospects of integration of nutrient-rich wastewater streams with microalgae cultivation, and McKetta (2002) and Pearlson (2011) outline techniques for assessing the impact of scaling chemical processes from pilot scale to commercial scale production. Finally, Wigmosta et al. (2011) and Florentinus (2008) quantify the potential for energy production from microalgae at the global and national scales. Wigmosta et al. (2008) employs a bottom-up approach for national bioenergy potential from microalgae and accounts for several growth constraints, but assumes the consumption of fresh water as a growth medium and the use of non-industrial CO_2 sources for growth supplementation. Florentinus et al. (2008) does not consider CO_2 constraints, and neglects many important geographic constraints such as land use and slope.

This thesis contributes to the existing literature in two ways. First, the potential for reductions in both production cost and lifecycle GHG emissions of microalgae-derived jet fuel is quantified for wastewater/aquaculture integration and facility scaling techniques. Second, the global energy potential of microalgae cultivated in open ponds is quantified with respect to water and CO_2 transportation requirements, geographic/climatic limitations, and industrial CO_2 availability while exclusively considering saltwater as the growth medium. Neither of these aspects has been addressed in existing literature on microalgae-derived jet fuel.

There are four chapters within this thesis: Chapter 2 outlines and describes the methods used in the analyses of wastewater/aquaculture integration and facility scaling impacts as well as the quantification of the global energy potential of microalgae-derived fuels. Chapter 3 summarizes the results of the four analyses and quantifies associated variability and uncertainty. Chapter 4 includes a summary of research completed, as well as discussion and conclusions drawn from the work.

[Page Intentionally Left Blank]

2 – Research Methods

2.1 – Impacts of Wastewater/Aquaculture Integration

Microalgae cultivation systems can be classified into two distinct categories: open raceway ponds and photobioreactors (PBRs). Open ponds consist of a large concrete bed in the shape of a racetrack. The growth medium is exposed to the environment, and a paddle wheel is used to provide circulation. Open ponds require the greatest amount of water input at 5.8 million gallons per day in the baseline scenario for a 137 BPD microalgae facility (Carter, 2012).

PBRs provide the ability to precisely control growth parameters and prevent contamination by invasive species (Carter, 2012), and they require very little water input relative to open ponds, ranging from 111,000 – 314,000 gallons per day in the baseline scenario for a 137 BPD microalgae facility (Carter, 2012). The technology types considered in this thesis include horizontal tubular, vertical tubular, and flat panel PBRs.

The cost of nutrients and a growth medium can constitute up to 30% of variable operating costs in open ponds and between 14 – 33% in PBRs in the most-likely (baseline) emission scenarios of the Carter 2012 analysis (Carter, 2012). Microalgae have been shown to consume the nutrients in municipal wastewater treatment (WWT) and aquaculture facilities that are otherwise removed through treatment processes (Woertz et al., 2009). Microalgae can also replace standard aeration processes in wastewater treatment (Freyberg, 2011). Integrating microalgae cultivation with WWT or aquaculture facilities may present an opportunity to obtain nutrients and a growth medium at little to no cost and displace GHG-intensive treatment processes, reducing overall production cost and lifecycle GHG emissions of microalgae-derived jet fuel.

Methods for integration between microalgae and wastewater/aquaculture facilities were designed to maximize total reductions in production cost and lifecycle GHG emissions of fuel. Figures 1 and 2 illustrate standard/integrated WWT and aquaculture processes, respectively, and the inputs displaced through integration. The resulting displaced inputs are described later in this section. In consistency with Carter (2012), the integrated facilities are assumed to utilize CO_2 from coal-fired power plants.

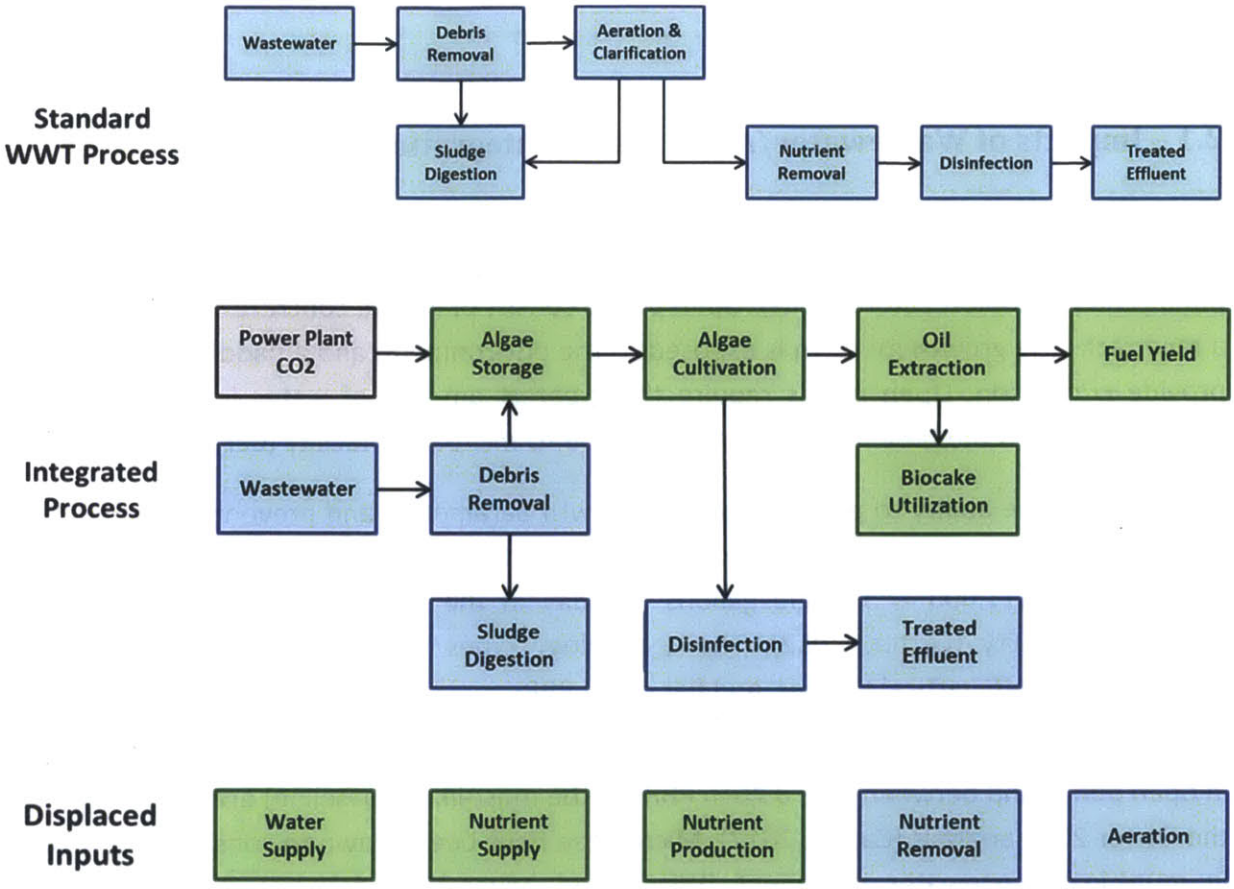

Figure 1 – Standard and Integrated WWT Processes with Displaced Inputs

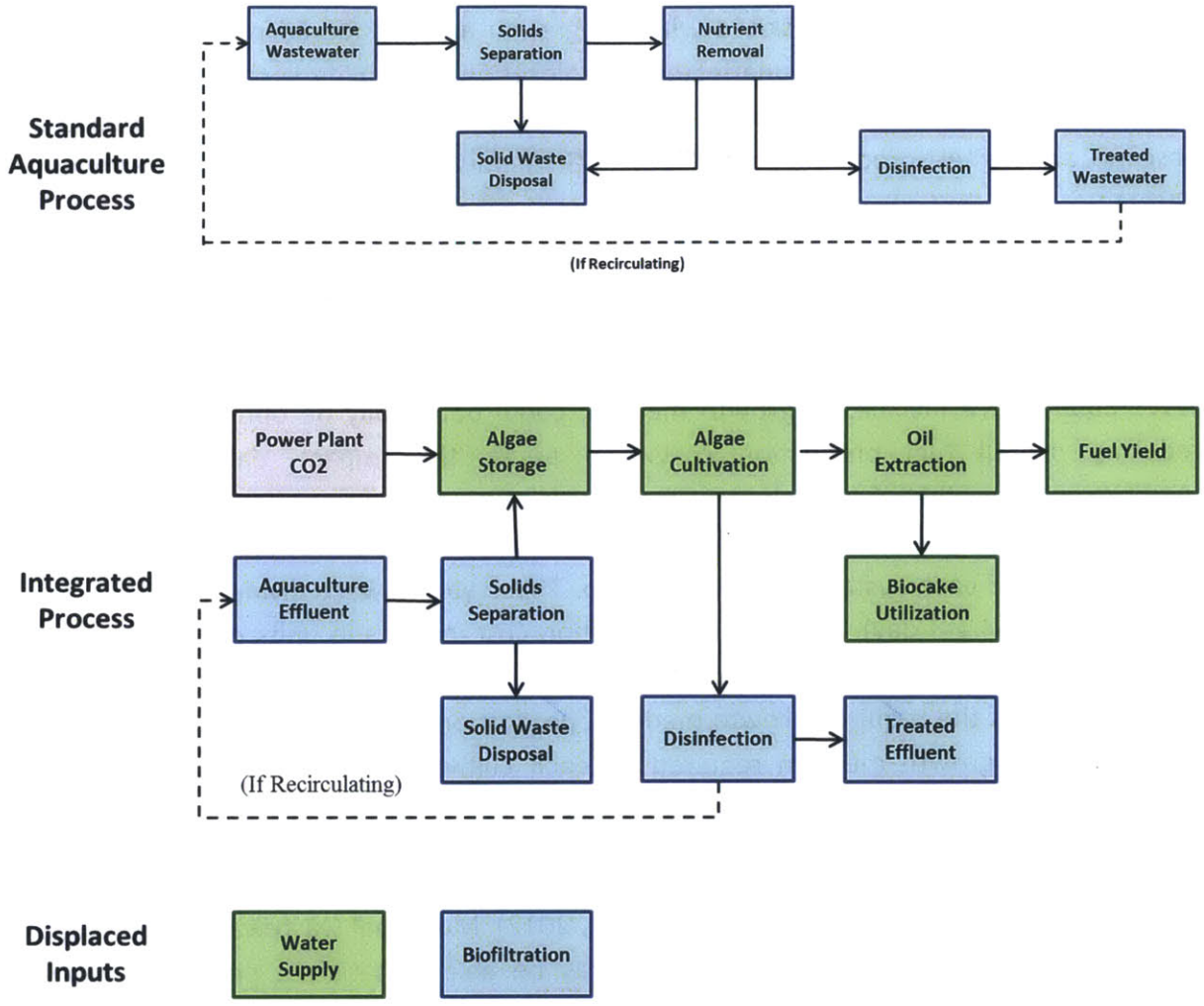

Figure 2 – Standard and Integrated Aquaculture Processes with Displaced Inputs

This analysis identifies the processes/inputs impacted via integration and quantifies the contribution of each to an overall reduction in production cost and/or lifecycle GHG emissions for fuel produced in a 137 BPD facility. Impacts were estimated for displaced inputs by multiplying the inputs by associated cost/emissions factors and dividing by the volumetric (with respect to production cost) or energy yield (with respect to GHG emissions) of the microalgae facility. Results are described in $\$/gal_{HEFA\text{-}J}$ and $gCO_2e/MJ_{HEFA\text{-}J}$ with respect to production cost and GHG emissions, respectively, and final integrated production cost and lifecycle GHG emissions of finished fuel are quantified for all scenarios and integration types.

Technology sets considered include open ponds, horizontal/vertical tubular PBRs, and flat panel PBRs (all technology sets assume wet extraction methods). All impacts derived via integration are allocated to the production of microalgae-derived jet fuel. This analysis assumes perfect colocation of microalgae and WWT/aquaculture facilities, and as such, transportation and

pumping costs/emissions associated with integration are considered negligible. Additionally, land costs are assumed to be unaffected by colocation. Variability is captured through three scenarios which consider technology sets and growth parameters resulting in the lowest, baseline, and highest production cost/lifecycle GHG emissions values in consistency with Carter (2012).

At $0.001/gal, the cost of the growth medium required for microalgae cultivation can impose significant fuel production costs, especially in open pond systems which require nearly 6 million gallons per day in the baseline scenario (Carter, 2012). Through integration with WWT/aquaculture facilities, a growth medium could potentially be obtained free of charge, reducing overall fuel production costs. To assess this impact, daily growth medium requirements for all four cultivation systems were taken from Carter (2012) and multiplied by the growth medium cost of $0.001/gal. See Table A1 in Appendix A for the growth medium requirements of each system in each scenario. These values were divided by daily fuel yield (137 BPD = 5754 gal/day), resulting in production cost impacts in units of $/gal$_{HEFA-J}$ for both integration types. Because it is assumed that WWT/aquaculture facilities are large enough to provide 100% of the required growth medium, production cost impacts correspond directly to the volume of growth medium required by each cultivation system. As such, impacts are identical between integration with WWT and integration with aquaculture.

The supply of nutrients required for microalgae cultivation can reach nearly 30% of the facility's total variable operational expenditures (Carter, 2012). Municipal wastewater and aquaculture mediums have high nutrient content, and may be able to satisfy a portion of microalgae nutrient requirements when imported as a growth medium (Woertz et al., 2009; Islam, 2005). Nutrient requirements per kilogram of algal biomass were assumed from Carter (2012) and multiplied by daily biomass production of 33,325 kg, resulting in total daily nutrient requirements.

Nutrient concentrations for municipal wastewater and aquaculture mediums were obtained from Carey & Migliaccio (2009) and Cripps & Bergheim (2000), respectively. Multiplying nutrient concentrations by the growth medium requirement of each system results in values for total daily nutrient availability from integration. See Table A2 for WWT and aquaculture nutrient concentration values in each scenario.

Values for cost of nutrients are given by Carter (2012), and were multiplied by total nutrient availability from integration to quantify total daily cost avoided. The results were divided by the daily fuel yield of the microalgae facility, resulting in fuel production cost impacts in $/gal$_{HEFA-J}$ for both integration types. When available nutrients exceeded nutrient requirements, values for nutrient requirements were considered in place of nutrient availability when dividing by facility fuel yield.

Nutrient production processes are often GHG-intensive (Wang, 2001). This analysis assumes that nutrients obtained through integration will no longer be produced, and as such, avoided emissions are allocated to finished fuel. Nutrient production emissions factors were assumed from Wang (2001) and multiplied by nutrient availability (or nutrient requirements as described previously) to quantify daily avoided emissions. Values were divided by facility energy yield (137 BPD ≈ 725,000 MJ/day), resulting in lifecycle GHG emissions impacts in $gCO_2e/MJ_{HEFA\text{-}J}$. See Table A3 for nutrients requirements, costs, and emissions factors assumed in each system/scenario.

WWT and aquaculture facilities continually employ treatment strategies to ensure that effluent streams meet environmental standards, particularly for nitrogen and phosphorus. Effluent discharge nutrient concentration regulations vary by state, but are often 15 mg/L or less for nitrogen and 2 mg/L or less for phosphorus (Jining & Junying, 2004). Microalgae have been documented to remove over 99% of total nitrogen and phosphorus resources available in municipal wastewater (Woertz et al., 2009). Through integration, many of these treatment processes can be displaced, and the resulting economic and environmental impacts may be allocated to finished fuel.

Three typical methods of nutrient removal in WWT facilities are considered in this analysis: the University of Cape Town/Virginia Initiative Plant (UCT/VIP) process, the Charlotte North Carolina (CNC) process, and the modified Orange Water and Sewer Authority (OWASA) process. Linden (2001) provides cost figures associated with each of these processes. It is assumed that microalgae can treat 100% of the growth medium imported from the WWT facility. Multiplying the daily cost of treatment processes by the growth medium requirements of each microalgae system results in daily treatment costs avoided. These values were then divided by daily fuel yield, resulting in fuel production cost impacts from displacing WWT processes in $\$/gal_{HEFA\text{-}J}$.

Additionally, WWT processes require inputs of electricity and acetic acid, which are associated with GHG emissions in their production. Linden (2001) describes electricity/acetic acid input requirements for each WWT process. Multiplying these values by daily growth medium requirements yields avoided daily electricity and acetic acid inputs.

Emissions factors for the production of acetic acid are assumed from Jones (2000), and are based on three production processes: the Monsanto process, the Cativa process, and biological production, in which all GHG emissions are biogenic. These emissions factors are used in high, baseline, and low scenario calculations, respectively. Multiplying emissions factors by avoided acetic acid requirements results in avoided daily GHG emissions. These values were divided by the microalgae facility energy yield to quantify emissions impacts in $gCO_2e/MJ_{HEFA\text{-}J}$. See Table A4 for nutrient removal costs, electricity/acetic acid input requirements, and emissions factors for acetic acid production.

An emissions factor for electricity is assumed from Wang (2001) at 626.54 gCO_2e/kWh, considering the U.S. pathway mix for electricity generation (this emissions factor is used in all electricity GHG calculations throughout this thesis). Multiplying avoided electricity requirements for WWT processes by this factor results in values for avoided daily GHG emissions, which are divided by the microalgae facility energy yield to quantify emissions impacts in $gCO_2e/MJ_{HEFA\text{-}J}$.

Aquaculture facilities typically employ biofiltration processes in place of the mechanical/chemical processes used in WWT facilities due to the relatively low nutrient concentration of aquaculture mediums. Emissions associated with biofiltration techniques are assumed to be 100% biogenic (Crab et al., 2007). As such, emissions impacts are not seen in displacing aquaculture treatment process. However, economic impacts may exist.

Aquaculture biofiltration cost figures are assumed from Crab et al. (2007) for three technologies: fluidized sand, bead filters, and trickling gravity filtration systems. These technologies are assumed in low, baseline, and high scenario calculations, respectively. Operating cost figures are given in units of $€/kg_{FISH}/yr$.

Nitrogen production per kilogram of fish raised is approximately 0.133 kg (Islam, 2005). Multiplying the biofiltration operating costs by this value results in operating costs in units of nutrient loads ($€/kg_{NITROGEN}/yr$) which, when multiplied by annual avoided nitrogen production from aquaculture integration (described previously) and converted to USD, results in total avoided biofiltration costs per year. These results were divided by annual fuel yield to quantify avoided biofiltration costs in $\$/gal_{HEFA\text{-}J}$. See Table A5 for original and converted biofiltration cost figures.

Finally, WWT facilities often employ aeration techniques in addition to nutrient removal strategies. These techniques, like nutrient removal processes, can be displaced through integration with microalgae facilities (Freyberg, 2011). The cost and emissions of aeration are attributable to electricity consumption. Freyberg (2011) cites an input requirement of 0.5 kWh/m^3 of water treated. This value was converted to kWh/gal of treated water and multiplied by the daily growth medium requirement of each system to calculate daily avoided electricity consumption from aeration. Resulting values were multiplied by cost figures and the electricity emissions factor to quantify daily avoided cost and GHG emissions (electricity cost values are assumed from the U.S. Energy Information Administration, see Table A6). Dividing avoided cost and avoided emissions by daily microalgae fuel and energy yield, respectively, resulted in economic and environmental impacts from displacing aeration in $\$/gal_{HEFA\text{-}J}$ and $gCO_2e/MJ_{HEFA\text{-}J}$.

The economic and environmental impacts derived from the displacement of each of the aforementioned inputs/processes were summed in each system for both integration types and

under all three variability scenarios. The final results quantify the total economic and environmental impact that may be achieved through the integration of microalgae and WWT/aquaculture facilities. Additionally, the results section includes values for integrated fuel production cost and lifecycle GHG emissions, which were quantified by subtracting total integration impacts from production cost and lifecycle GHG emissions values given in Carter (2012).

2.2 – Impacts of Scaling

Certain fixed/variable operating costs and inputs, as well as some capital costs, may not scale linearly as the fuel yield of the microalgae facility is increased from pilot to commercial scale. Scaling could serve as an additional strategy for reducing cost and lifecycle GHG emissions of microalgae-derived jet fuel. This analysis identifies and quantifies impacts from aspects affected by scaling the microalgae facility from a pilot-scale yield of 137 BPD to a commercial-scale yield of 2192 BPD (16 times larger). The cost/emissions contribution of each aspect is assessed in both pilot and commercial-scale scenarios (in the same metrics as Section 2.1) by multiplying required inputs by cost/emissions factors. The differences between pilot and commercial results represent the reduction in cost/emissions that may be achieved through scaling.

It is assumed that the layout of the commercial-scale facility is identical to the pilot-scale facility, and that components are simply scaled to produce 2192 BPD. Thus, no additional linkages or components are considered. This analysis is executed only for open raceway pond cultivation systems using a wet extraction technique. Variability is captured through three scenarios which consider technology sets and growth parameters resulting in the lowest, baseline, and highest production cost/lifecycle GHG emissions values in consistency with Carter (2012). Additionally, impacts from wastewater/aquaculture integration are combined with impacts from scaling to assess the maximum achievable reductions in fuel production cost and lifecycle GHG emissions.

Staffing costs can constitute more than 25% of fixed operating expenses in certain open pond scenarios (Carter, 2012), and have been shown to scale in a non-linear fashion (Pearlson, 2011). The number of required employees and the average salary per employee for a 137 BPD microalgae facility are outlined in Carter (2012). Multiplying the number of employees by average salary and dividing by the annual plant yield in gallons results in staffing's contribution to total production cost at pilot scale. This metric is calculated at the commercial scale in the same manner. However, the number of required employees does not scale linearly.

Three existing/conceived microalgae cultivation/harvesting/extraction facilities were observed, and number of employees versus fuel yield was plotted in order to empirically relate number of

employees to yield. A trend line was fitted to the data, and the resulting equation was used to estimate number of employees required by a 2192 BPD facility (see Figure A1). This number was then used to calculate staffing's contribution to total production cost at commercial scale (low and high scenarios consider a ±25% deviation from the calculated number of employees). The difference between staffing costs at the commercial and pilot scales represents an economic impact of scaling. See Table A7 for staffing requirements and salaries in pilot and scaled facilities.

In the baseline scenario, upgrading algal oil to finished fuel constitutes over 10% of variable operating expenses (Carter, 2012). Upgrading is outsourced to a dedicated facility, and the capacity of the upgrading facility influences upgrading cost (Pearlson, 2011). Upgrading facilities of 6500 BPD, 4000 BPD, and 2000 BPD capacity are considered in the low, baseline and high scenarios of Carter (2012) and associated upgrading costs are presented in $\$/gal_{OIL}$. Upgrading costs were plotted against upgrading capacity, and a trend line was fitted to the data. The resulting equation was used to estimate upgrading costs in high-capacity upgrading facilities (see Figure A2).

The capacity of the upgrading facility used by the commercial-scale microalgae facility is assumed to scale by 3 in the low scenario, 4 in the baseline scenario, and 5 in the high scenario. It is therefore assumed that the 2192 BPD microalgae facility employs upgrading plants of 19,500 BPD, 16,000 BPD, and 10,000 BPD capacity in the low, baseline, and high scenarios, respectively. The difference in upgrading costs at the pilot and commercial scales represents another economic impact of scaling. See Table A8 for upgrading facility capacity assumptions and corresponding upgrading costs.

Utility input requirements (such as electricity) do not scale linearly as a result of proportionally lower losses in higher-capacity equipment (Bonaquist, 2013). Scaling the microalgae facility may reduce the quantity of electricity required per $kg_{BIOMASS}$, potentially resulting in reduced production cost and lifecycle GHG emissions. Equation 1 is derived from McKetta (2002),

$$Cost_2 = Cost_1(16)^R \qquad (1)$$

and allows the cost/quantity of a scaled input or component ($Cost_2$) to be estimated based on the known cost/quantity of an original input/component ($Cost_1$), the scaling factor (16 for the commercial-scale facility), and the scaling exponent (R), which is given for several components and inputs.

Specific energy use values for cultivation, harvesting and extraction processes are presented in Carter (2012) in units of $MJ/kg_{BIOMASS}$ (see Table A9). Summing these values and multiplying by a

required biomass input of 33,325 kg/day (Carter, 2012) resulted in energy consumption per day in the 137 BPD facility. Only energy inputs from electricity were considered, as chemical inputs have a scaling exponent of 1.0 (McKetta, 2002). The resulting value represents $Cost_1$ in Equation 1. $Cost_2$ was then calculated considering a scaling exponent for electricity of 0.65 (McKetta, 2002), and is the quantity of electricity required per day in a 2192 BPD microalgae facility. Results were then converted from MJ to kWh.

Daily electricity requirements for pilot and commercial-scale plants were multiplied by cost and emissions factors to quantify the production cost and lifecycle GHG emissions attributable to electricity consumption of cultivation, harvesting, and extraction processes. Electricity costs range from \$0.08 – 0.17/kWh (U.S. Energy Information Administration, 2014). \$0.13/kWh is assumed in the baseline scenario. An emissions factor for electricity of 626.54 gCO_2e/kWh is assumed from Wang (2001) with respect to the U.S. pathway mix for electricity generation, which considers the weighted average GHG emissions of electricity from all generation sources.

The resulting cost and emissions quantities were divided by daily fuel/energy yield, reducing the results to $\$/gal_{HEFA-J}$ and gCO_2e/MJ_{HEFA-J}, respectively. The differences between pilot and commercial-scale results represent an additional economic impact of scaling and the singular environmental impact of scaling.

In the baseline scenario, capital costs may constitute up to 50% of total fuel production costs. Additionally, cultivation, harvesting, and extraction equipment are responsible for the majority of capital costs in open pond systems (Carter, 2012). Table 1 describes the cultivation, harvesting, and extraction components in open pond cultivation systems for each scenario.

Table 1 - Cultivation, Harvesting, and Extraction Components Used in Open Pond Systems (Carter, 2012)

Baseline Components	Low Components	High Components
Open Ponds	Open Ponds	Open Ponds
CO2 Feed System	Water/Nutrient/Waste System	CO2 Feed System
Water/Nutrient/Waste System	Paddle Wheels	Water/Nutrient/Waste System
Paddle Wheels	Settling Ponds	Paddle Wheels
Clarifiers	Anaerobic Digester	DAFs
Anaerobic Digester	CHP Unit	Belt Filter Press
CHP Unit		Anaerobic Digester
		CHP Unit

Installed capital costs for pilot-scale components are given in Carter (2012) in a $\$/MJ_{HEFA-J}$ metric and were converted to daily costs through multiplying by plant energy yield. Daily cost values were then used in Equation 1 with appropriate scaling exponents for equipment from McKetta (2002) to calculate commercial-scale daily cost values for each component. The scaling exponent for CHP units was obtained from the U.S. Department of Energy (National Energy Technology Laboratory, 2013). Pilot and commercial-scale daily cost values were reduced to $/gal by dividing by daily fuel yield. The difference between them represents the final economic impact of scaling.

Components without provided scaling exponents were assigned the scaling exponent of the physically closest matching component (see Table A10). For scaling exponents with ranges, low values and high values are assumed in the low and high scenario calculations, respectively, with the average assumed in the baseline scenario. See Table A11 for component capital costs and scaling exponents.

The economic and environmental impacts derived from scaling were summed in each system under all three variability scenarios. The final results quantify the total economic and environmental impact that may be achieved through scaling of microalgae facilities. Additionally, the results section includes values for scaled fuel production cost and lifecycle GHG emissions, which were quantified by subtracting total scaling impacts from production cost and lifecycle GHG emissions values given in Carter (2012). As this analysis assumes that impacts from wastewater/aquaculture integration and scaling are mutually exclusive, economic and environmental impacts from both analyses were summed in order to quantify the maximum achievable reduction in fuel production cost and lifecycle GHG emissions. The results of this analysis are included in the results section of scaling impacts.

2.3 – Global Bioenergy Potential of Microalgae

The annual energy yield of a given area can be calculated by multiplying the annual areal energy yield by the amount of area available for crop cultivation and subsequently considering growth medium and CO_2 availability limitations. Quantification of the annual global bioenergy potential of HEFA-J derived from microalgae is achieved through a summation of the annual energy yields of finite elements or "cells". The energy yield of any given cell is a function of biological parameters, climatic parameters (which are variable over time and location), and land/CO_2 constraints. Equation 2 has been developed for calculating annual global bioenergy potential of microalgae biomass,

$$E_G = \sum_{i=0}^{n} \varphi_i \, A_i \, c_i \qquad (2)$$

where E_G is the annual global bioenergy potential of biomass, φ_i is the areal energy yield of a cell, A_i is the available cultivation area of the cell, and c_i is the carbon dioxide saturation coefficient of the cell. The variable n is the total number of cells, or approximately 7.4 million in this analysis. This analysis captures variability by quantifying bioenergy potential in three scenarios, which assume biological/physical characteristics and constraints resulting the lowest, baseline, and highest global bioenergy potential.

Equation 3 was used to calculate annual areal energy yield (φ),

$$\varphi = (0.214)(\tau_p)(C_{PAR})(\varepsilon_t)(\varepsilon_s)(E_s) \qquad (3)$$

and follows the biophysical model of Wigmosta (2011) which has been used in scientific literature to calculate the energy potential of microalgae on a national scale.

In Equation 3, τ_p is the transmission efficiency of solar radiation, C_{PAR} is the fraction of photosynthetically active radiation, ε_t is the growth medium temperature correction factor, ε_s is the light utilization efficiency of microalgae, and E_s is the full-spectrum solar energy present at the earth's surface in units of J/m^2/s.

The transmission efficiency of solar radiation to microalgae and the average fraction of photosynthetically active radiation delivered by the sun are well-established and can be considered constant, at 0.90 and 0.46, respectively (Wigmosta et al., 2011). However, ε_t, ε_s, and E_s are dependent on climatic parameters. All values were calculated at a high geographic and temporal resolution in order to improve accuracy and reliability. See Appendix B for equations used in calculating ε_t and ε_s.

Sea surface temperature (SST) data used in calculating ε_t and ε_s was obtained from the National Oceanographic Data Center's Pathfinder database. Insolation data representing E_s and used in calculating ε_s was obtained from NASA's Atmospheric Science Data Center. As ocean water exclusively is used as the growth medium, the water temperature value assigned to each analyzed cell is equal to the geographically nearest available SST data.

SST and insolation data were imported into ArcGIS for processing at a geographical resolution of 5 arc minutes and a temporal resolution of one month. Values for ε_t and ε_s were calculated

for each cell for each month of data, and Equation 3 was employed with the results to determine the areal energy yield of each cell for each month. Through summation of the results of all 12 months, an annual areal energy yield (φ) was computed for each cell in units of MJ/yr.

The Global Agro-Ecological Zones (GAEZ) model was used to identify land that is assumed to be unavailable for energy crop cultivation, as it is already being used for other purposes or is of particularly high environmental value. In particular, built-up land (developed urban and rural areas), land currently used for agricultural purposes, and natural forests/protected habitats are excluded from this analysis (Fischer & Schrattenholzer, 2001).

The data from this model is given as the fraction of marginal land within a cell at a resolution of 5 arc minutes (see Figure A3). Available cultivation area (A) is computed by multiplying the percentage of marginal land in each cell by the total area of the cell (5 arc minutes $\approx$ 10 kilometers).

The annual areal energy yield of each cell was multiplied by the cell's available cultivation area to produce maximum annual energy yield (φ_{BIO}) estimates in units of $kg_{BIOMASS}$/yr, which may be achievable with 100% CO_2 supplementation. However, industrial CO_2 is unavailable in certain areas, and in many cases is not available in the quantities required to achieve maximum microalgae growth in a cell. As such, CO_2 saturation coefficients were computed for each cell to determine the maximum amount of microalgae growth that can be supplemented by the industrial CO_2 available to the cell.

This analysis assumes that microalgae will only be cultivated if industrial CO_2 is available for supplementation. The Platts World Electric Power Plants Database was used to plot the geographic location and generation capacity of all operating coal-fired and natural gas power plants throughout the world. Termuehlen & Emsperger (2003) evaluate the amount of CO_2 produced per kWh of electricity produced in a coal-fired power plant, which varies with plant efficiency. These values were converted into a kg_{CO2}/day/MW metric and extrapolated to encompass efficiencies ranging from 25 – 60%. Based on stoichiometry, natural gas produces 50.47% as much CO_2 versus coal in the generation of equal amounts of power (U.S. EPA, 2014).

The efficiency of coal-fired power plants ranges from 25% for subcritical plants to 45% for state-of-the-Art plants, with a global average efficiency of 33% (World Coal Association, 2014). With respect to natural gas plants, efficiencies range from 35% in simple cycle plants to 60% in combined cycle plants, with a global average of 45% (American Electric Power, 2012). Table 2 outlines the power plant efficiencies assumed in low-constraint, baseline, and high-constraint scenarios. See Figure A4 for CO_2 production rates per MW versus plant efficiency for coal-fired and natural gas power plants.

Table 2 - Coal and Natural Gas Power Plant Efficiencies Assumed in Low, Baseline, and High Scenarios

Scenario	Coal Efficiency	NG Efficiency
Low	25%	35%
Baseline	33%	45%
High	45%	60%

The resulting values derived from Termuehlen & Emsperger (2003) for coal-fired and natural gas power plants were used as conversion factors and multiplied by power plant capacity in MW to determine the rate of CO_2 production of each power plant in kg_{CO2}/day, and this data was plotted in ArcGIS. Annual CO_2 production was calculated by multiplying by 365 days, and the results were aggregated to a resolution of 200 kilometers to facilitate calculations with respect to CO_2 transportation constraints.

CO_2 requirements for microalgae cultivation are 2.43 $kg_{CO2}/kg_{BIOMASS}$, 2.05 $kg_{CO2}/kg_{BIOMASS}$, and 1.93 $kg_{CO2}/kg_{BIOMASS}$ in the low-constraint, baseline, and high-constraint scenarios, respectively, assuming a CO_2 fixation efficiency of 90%, with the remaining 10% escaping into the atmosphere through outgassing (Carter, 2012). CO_2-constrained annual biomass production values (φ_{CO2}) were calculated for each 200 km region by multiplying CO_2 requirements by available CO_2 in the region. Multiplying by the energy content of microalgae biomass (32.8 $MJ/kg_{BIOMASS}$) results in CO_2-constrained annual energy yield (φ_{CO2}) values for each region in units of MJ/yr (Carter, 2012).

φ_{BIO} yield values were aggregated to a 200 km resolution in ArcGIS for consistency with φ_{CO2} values. CO_2 saturation coefficients were then calculated for each region using Equation 4:

The result for each region is capped at a maximum of 1.0, and is assigned to all cells with the region for further calculations. Through the application of CO_2 saturation coefficients, the annual energy yield of a cell is constrained when the available quantity of CO_2 is insufficient for maximum growth.

Through Equation 2, the product of annual areal energy yield, available cultivation land, and CO_2 saturation constant values for each included cell are summed globally to produce estimates for the annual global bioenergy potential of microalgae biomass. The result for each scenario is

then multiplied by the extractable lipid fraction of microalgae to calculate the annual global bioenergy potential of microalgae oil (see Table A12 for assumed extractable lipid fractions). Finally, global energy potential of microalgae oil is multiplied by the maximum jet product slate share of HEFA-J after upgrading in order to produce final results for annual global bioenergy potential of microalgae-derived HEFA-J. The maximum-jet product slate share for HEFA-J is assumed to be 49.4% (Carter, 2012). Many cells are excluded in this calculation with respect to the assumptions described henceforth.

CO_2 transportation from power plants to microalgae facilities should not exceed 200 kilometers for economic and environmental reasons (Global CCS Institute, 2012). As such, all cells greater than 200 kilometers from an industrial CO_2 source are excluded from this analysis.

Growth medium transportation does not exceed 100 miles in order to maintain pumping costs below $\$0.50/gal_{HEFA\text{-}J}$. Since saline water is considered exclusively as the growth medium in this analysis, all cells greater than 100 miles from a major saline water body are excluded in calculations. This threshold was selected with respect to the results of an economic pumping analysis, as described in Appendix C, and is similar in magnitude to the value assumed by Florentinus et al. (2008), which assumes a maximum water transportation distance of 100 kilometers (62 miles).

Land slope does not exceed 2% for economic reasons (Muhs et al., 2009; Benemann et al., 1982). Data from the Advanced Spaceborne Thermal Emission and Reflection Radiometer (ASTER) Global Digital Elevation Map was imported into ArcGIS, and slope values were computed for each cell through the ArcGIS slope function at a resolution of 5 arcminutes. All cells with a value greater than 2% were excluded from calculations.

The following assumptions affect cell energy yield calculations, but do not exclude any cells from calculations. It is assumed that cultivation facilities operate 365 days per year. However, recent work has indicated that 3-season operation may be effective in reducing the lifecycle emissions of produced fuel with an associated decrease in annual energy yield (Davis et al., 2014).

Biological/physical characteristics and input requirements of microalgae strains are highly variable. With respect to consistency, values for these characteristics have been assumed directly from the work of Carter (2012) and Wigmosta et al. (2011). See Table A12 for a summary of assumed values for global variables used in the calculations of the preceding sections.

3 – Results

3.1 – Wastewater Integration

The overall production cost impact on microalgae-derived HEFA jet fuel from integration with municipal WWT facilities is comprised of economic impacts from the displacement of required water/nutrient inputs, in addition to the fuel production facility's capacity for displacing aeration and nutrient removal processes. Figure 3 illustrates the production cost impacts for each WWT-integrated microalgae cultivation system in the baseline scenario. In addition to the overall production cost impact, each displaced input and its respective contribution to the overall economic impact is identified.

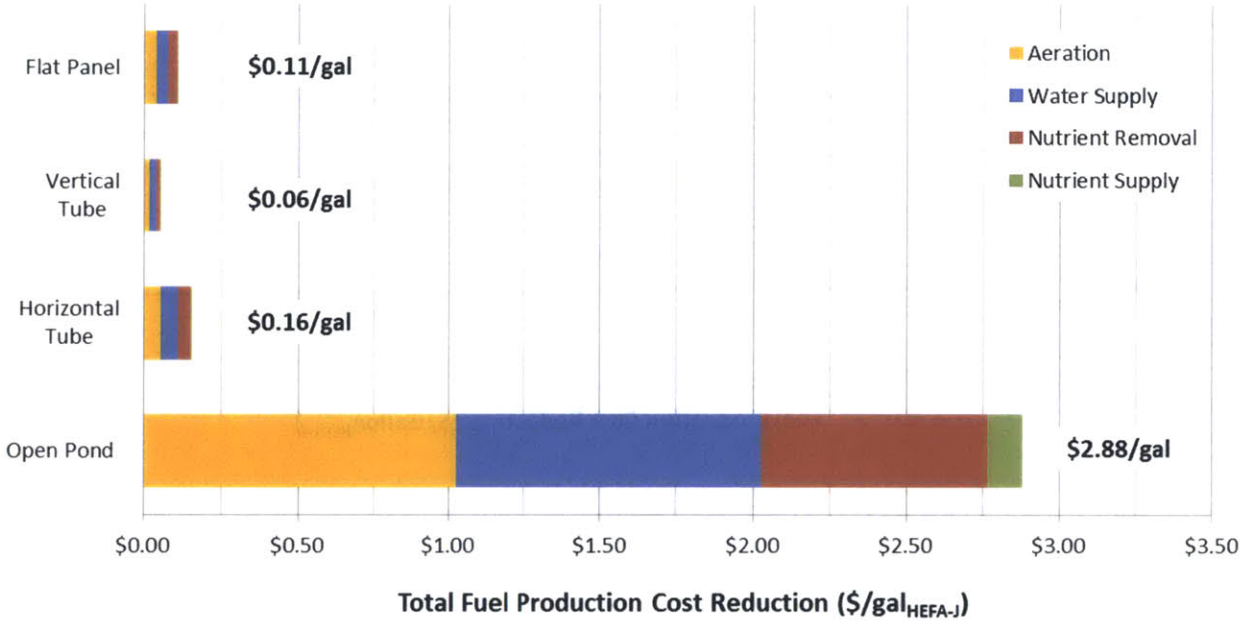

Figure 3 – Baseline Economic Impacts from Integration with Wastewater Treatment

Open pond cultivation systems are affected most by WWT integration, reducing fuel production costs by \$2.88/gal$_{HEFA-J}$ or 29.2%. Impacts in PBR systems are an order of magnitude lower, ranging from \$0.06 – 0.16/gal$_{HEFA-J}$, or less than 1% in all systems.

Aeration displacement results in the greatest economic impact, reducing fuel production cost by \$1.02/gal$_{HEFA-J}$ in the open pond system. An additional \$1.00/gal$_{HEFA-J}$ is saved by growth medium displacement, and the displacement of nutrient removal processes reduces production

cost by an additional $0.74/gal$_{HEFA-J}$. Finally, displacing required nutrient inputs results in a $0.11/gal$_{HEFA-J}$ reduction in production cost.

Variability captured throughout this study results in a range of potential economic impacts for each integrated microalgae cultivation system. Figure 4 describes these ranges, where green tick marks represent baseline reduction in production cost, with the variability bars representing low and high-scenario production cost impacts.

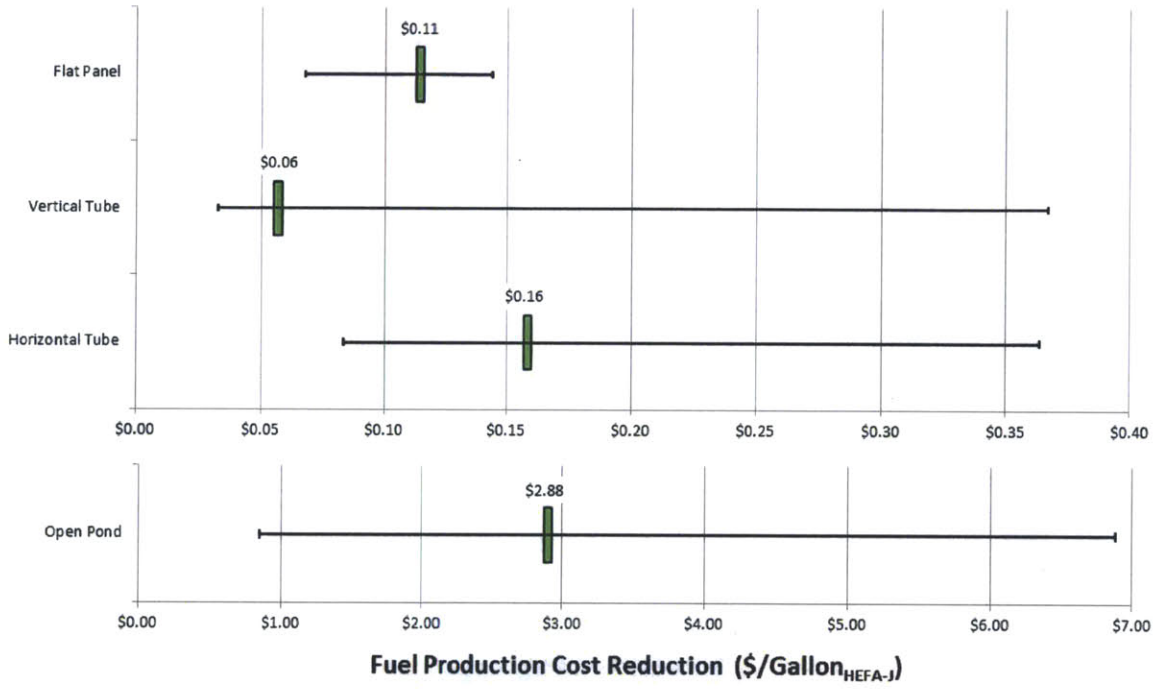

Figure 4 – Variability of Production Cost Impacts from Wastewater Integration

Fuel production cost impacts range from $0.03 - $0.36/gal$_{HEFA-J}$ in PBR systems, and from $0.75 – 6.83/gal$_{HEFA-J}$ in open pond systems. It should be noted that maximum cost impacts may not be achievable in baseline systems, as these values are calculated for high-scenario systems from Carter (2012) which require greater economic inputs.

Finally, Figure 5 compares the ranges of fuel production cost for non-integrated (assumed from Carter 2012) and WWT-integrated microalgae cultivation systems. Variability of integration impacts is included in the results illustrated by Figure 5.

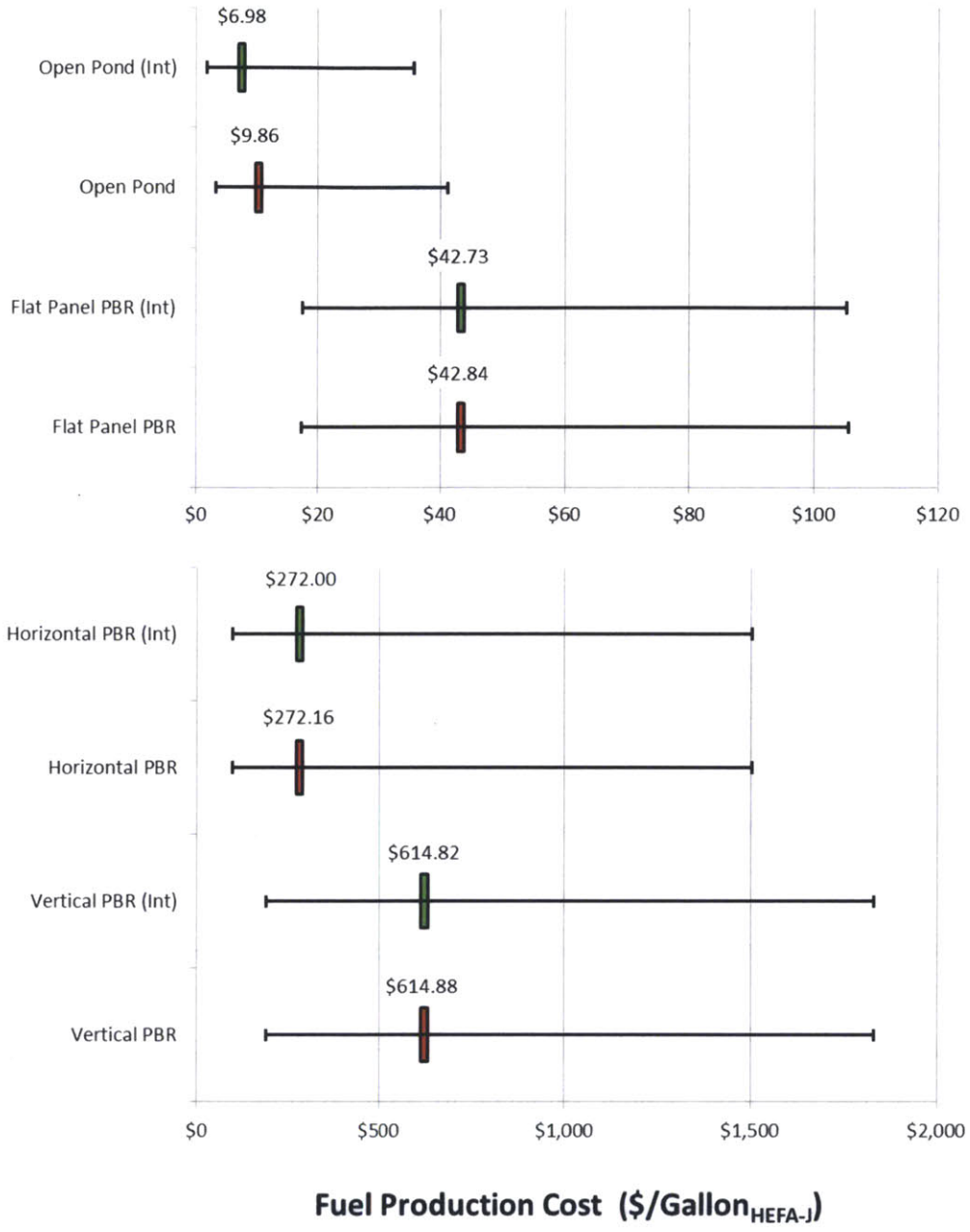

Figure 5 – Range of Total Fuel Production Costs of Standard and WWT-Integrated Microalgae Cultivation Facilities

Total lifecycle emissions impacts are the combined result of reductions due to the displacement of acetic acid/nutrient production and aeration/nutrient removal processes. Figure 6 illustrates the lifecycle emissions impacts for each WWT-integrated microalgae cultivation system in the

baseline scenario. In addition to the overall lifecycle emissions impact, each displaced input and its respective contribution to the overall emissions impact is identified.

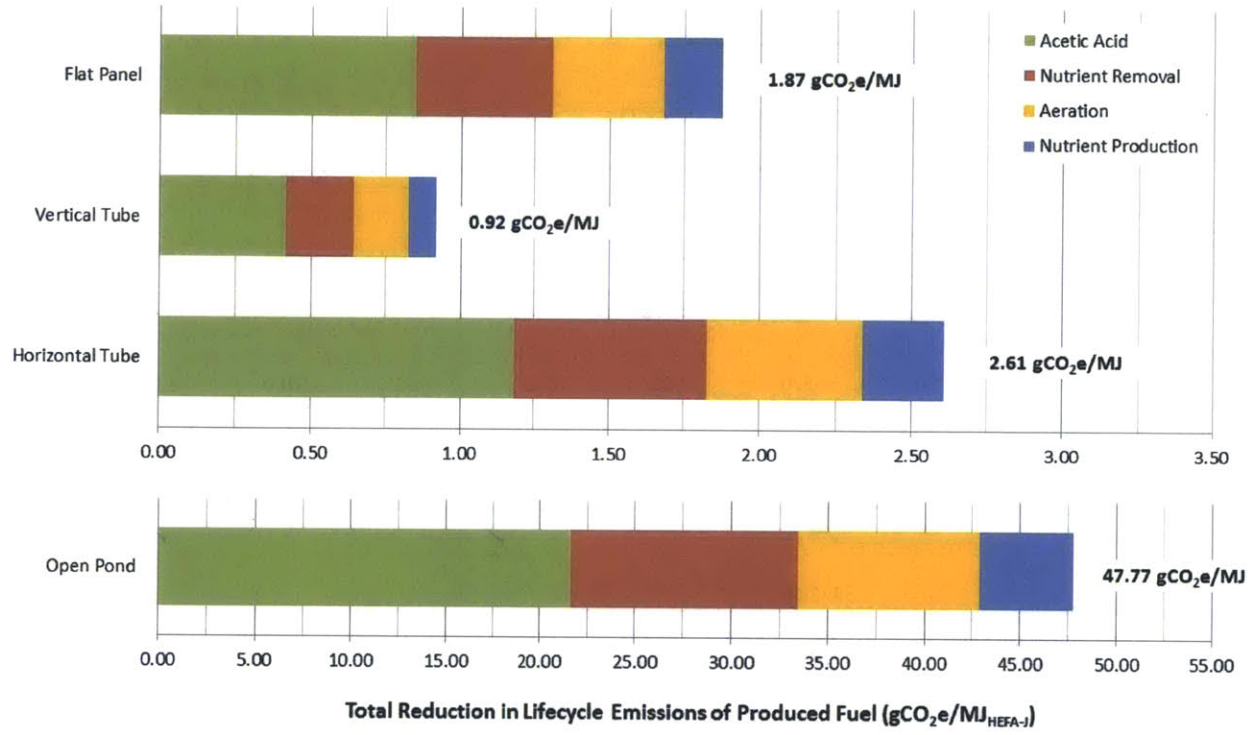

Figure 6 – Baseline Total Lifecycle Emissions Reductions of Produced Fuel from WWT Integration

Emissions impacts from WWT integration are greatest for open pond systems at 47.77gCO_2e/MJ_{HEFA-J}, or over 100%. Impacts in PBR systems range from 0.92 – 2.61 gCO_2e/MJ_{HEFA-J}.

Displacement of acetic acid production results in the greatest individual emissions impact at 21.65gCO_2e/MJ_{HEFA-J} in the open pond system, followed by displacement of nutrient removal at 11.77gCO_2e/MJ_{HEFA-J}. Displacing aeration processes reduces lifecycle emissions by 9.42gCO_2e/MJ_{HEFA-J}, and an additional 4.93 gCO_2e/MJ_{HEFA-J} is avoided through displacement of nutrient production.

Figure 7 describes the ranges of lifecycle emissions reduction potential considering captured variability, where green tick marks represent baseline reduction in lifecycle emissions, with the variability bars representing low and high-scenario emissions impacts.

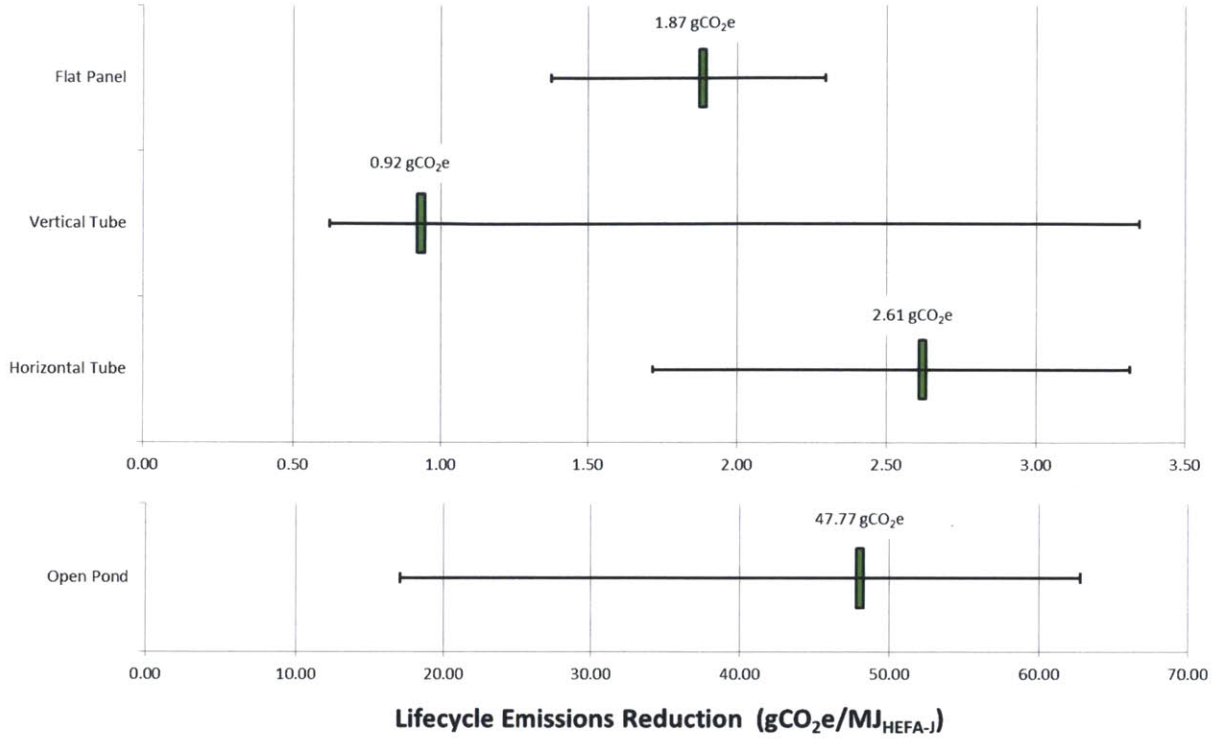

Figure 7 – Variability of Lifecycle Emissions Impacts from Wastewater Integration

Lifecycle emissions impacts range from 0.57 – 3.35 gCO_2e/MJ_{HEFA-J} in PBR systems, and from 16.07 – 62.77 gCO_2e/MJ_{HEFA-J} in open pond systems. Again, maximum emissions impacts may not be achievable in baseline systems, as these values are calculated for high-scenario systems from Carter (2012) which require greater energy and material inputs.

Figure 8 compares the ranges for lifecycle emissions of produced fuel in non-integrated (assumed from Carter 2012) and WWT-integrated microalgae cultivation systems. Variability of integration impacts is included in the results.

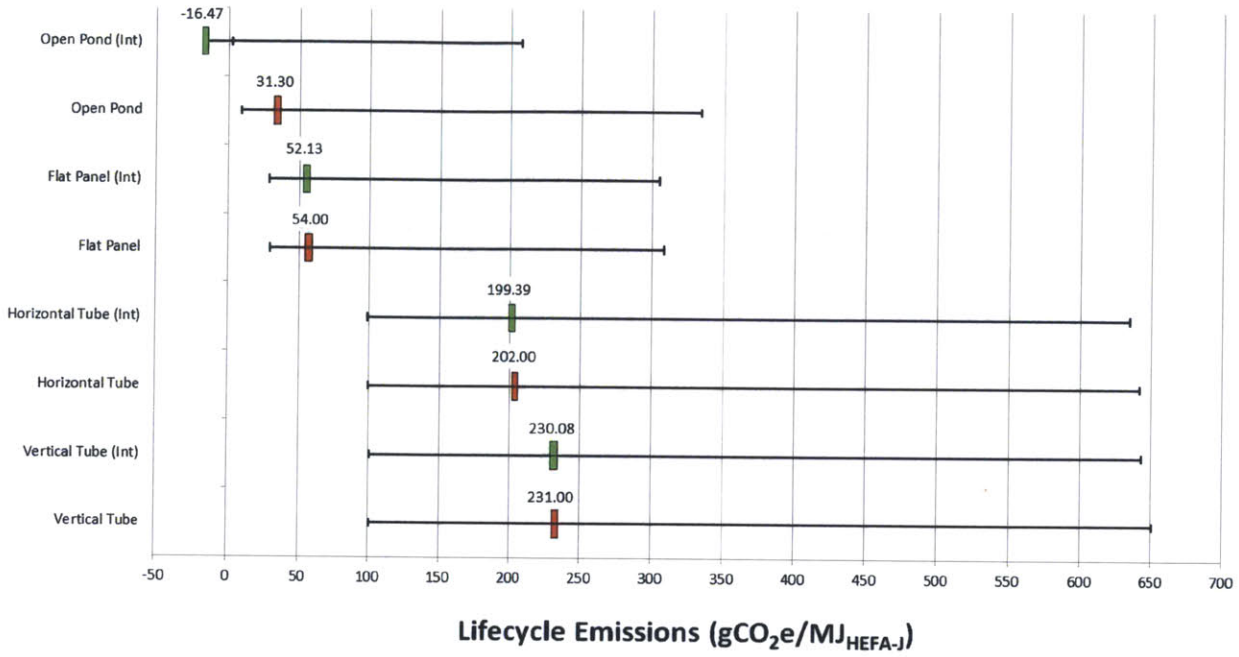

Figure 8 – Range of Total Fuel Lifecycle Emissions of Standard and WWT-Integrated Microalgae Cultivation Facilities

It should be noted that the lifecycle emissions in the baseline scenario integrated open pond system are lower than the low scenario for the same system due to the greater emissions impacts resulting from integration in the baseline scenario.

3.2 – Aquaculture Integration

The overall production cost impact on microalgae-derived HEFA jet fuel from integration with aquaculture facilities is comprised of economic impacts from the displacement of required water inputs and the displacement of biofiltration processes. Figure 9 illustrates the production cost impacts for each aquaculture-integrated microalgae cultivation system in the baseline scenario.

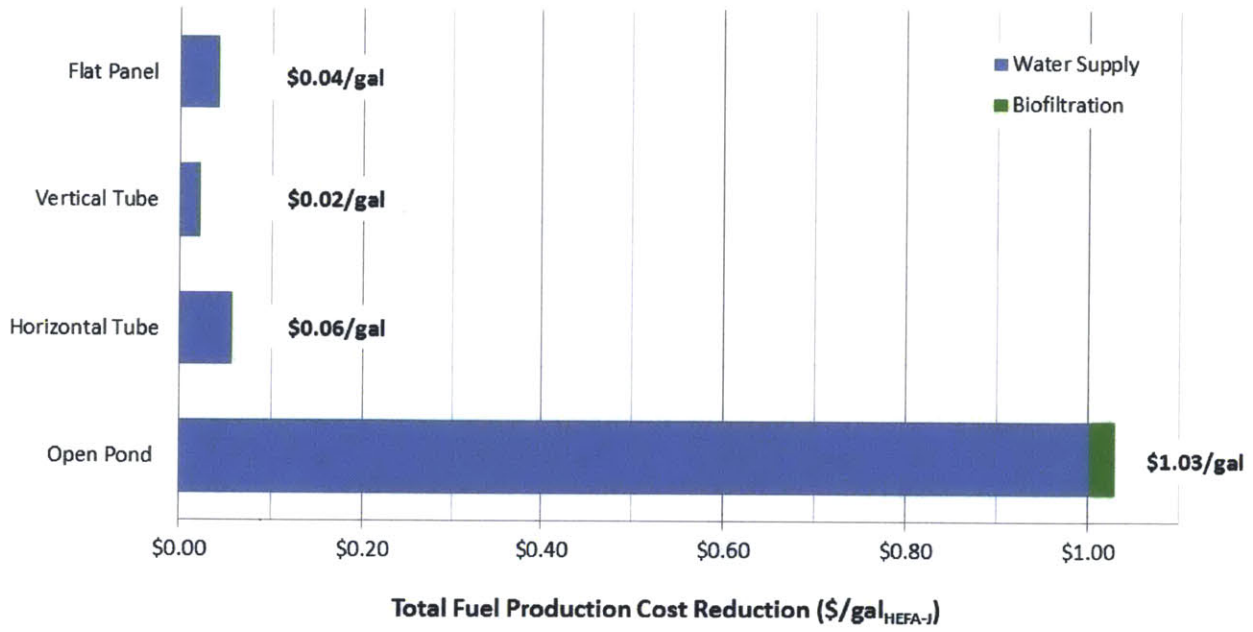

Figure 9 – Baseline Total Fuel Production Cost Reductions from Integration with Aquaculture Facilities

Production cost impacts range from \$0.02 – 0.06/gal$_{HEFA-J}$ or less than 1% in baseline PBR systems. Production cost in baseline open pond systems is reduced by \$1.03/gal$_{HEFA-J}$, or 10.4%. Water supply displacement is largely responsible for reductions in fuel production cost, constituting 97.1% of overall impact in each scenario.

Variability in potential economic impacts captured throughout this portion of the study is described by Figure 10. In PBR systems, production cost impacts range from \$0.01 – 0.15/gal$_{HEFA-J}$. In open pond systems, impacts range from \$0.27 – 2.72/gal$_{HEFA-J}$.

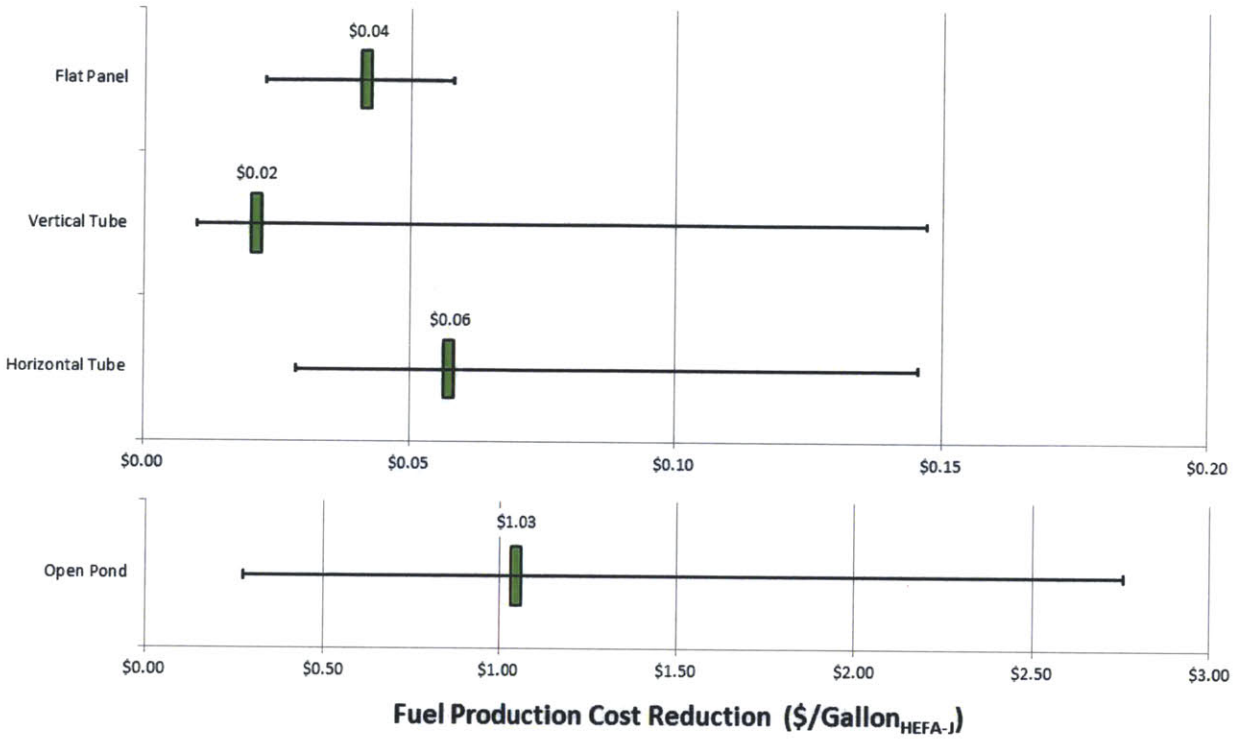

Figure 10 – Variability of Production Cost Impacts from Aquaculture Integration

Figure 11 compares the ranges of fuel production cost for non-integrated and aquaculture-integrated microalgae cultivation systems. Variability of integration impacts is included in these results.

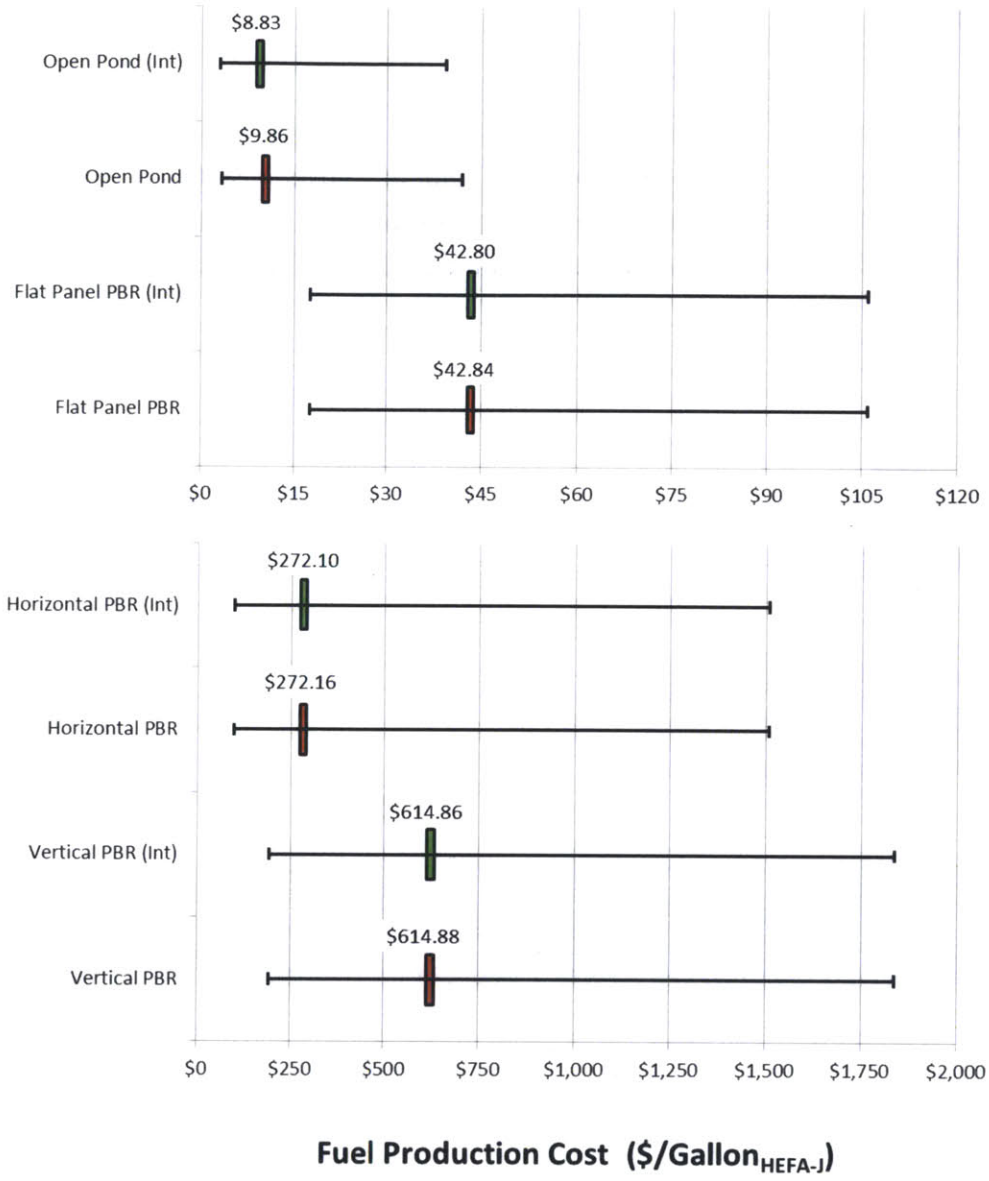

Figure 11 – Total Fuel Production Costs of Standard and Aquaculture-Integrated Microalgae Cultivation Facilities in Baseline, Low, and High Scenarios

Production cost impacts from aquaculture integration are derived solely from the displacement of nutrient production. Emissions avoided due to nutrient production were negligible in all systems/scenarios at a maximum of less than 0.5% reduction in lifecycle emissions. As such, lifecycle emissions in aquaculture-integrated systems are assumed to be identical to those given by Carter (2012).

3.3 – Scaling

Production cost impacts resulting from scaling a 137 BPD open pond facility to a yield of 2192 BPD are comprised of reductions in capital costs, staffing requirements, and electricity/upgrading costs. Figure 12 describes the total fuel production cost impact of scaling in each scenario for an open pond system, and each identified impact's contribution to the overall impact.

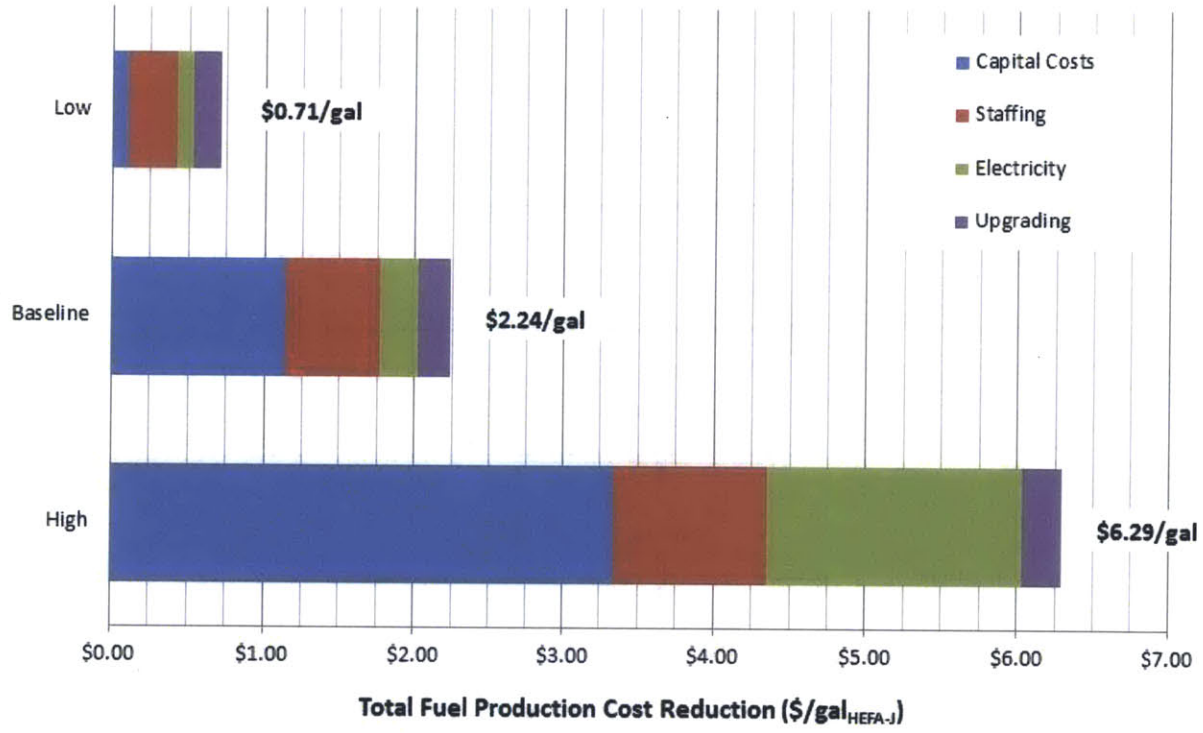

Figure 12 – Total Fuel Production Cost Reduction from Scaling 137 BPD Facility to 2192 BPD

Production cost impacts range from \$0.71 – 6.29/gal_{HEFA-J} as a result of scaling, with an impact of \$2.24/gal_{HEFA-J} in the baseline scenario, or 22.7%. Reductions due to capital costs result in the greatest impact in baseline and high scenarios, and reductions due to staffing costs dominate in the low scenario due to lower initial capital costs assumed in the low scenario.

Reducing the relative capital costs of operation via scaling yields a reduction in fuel production cost of \$1.14/gal_{HEFA-J} in the baseline scenario, or 50.9% of the overall impact of scaling. An additional \$0.63/gal_{HEFA-J} is saved in the form of staffing costs, and \$0.25/gal_{HEFA-J} is avoided due to reduced electrical consumption of cultivation, harvesting, and extraction equipment. Finally, a cost reduction of \$0.22/gal_{HEFA-J} is the result of scaling upgrading processes.

Figure 13 illustrates the resulting production cost of fuel in a 2192 BPD facility against that of a standard 137 BPD facility. Variability in the economic impacts of scale is included with the variability in fuel production cost outlined in Carter (2012).

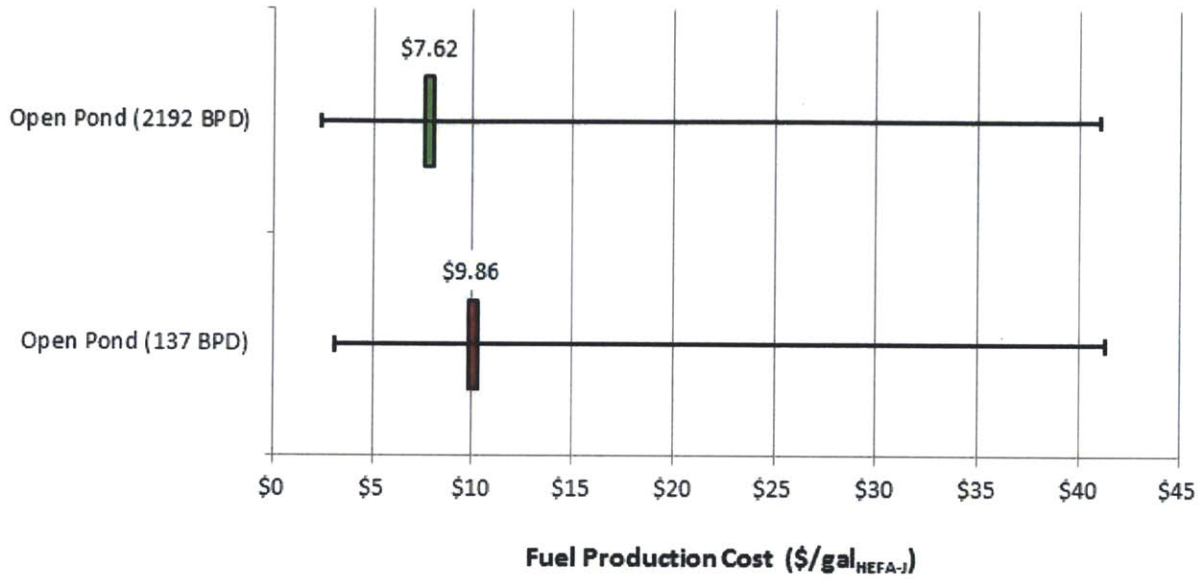

Figure 13 – Fuel Production Costs for Pilot and Commercial Scale Facilities

Reducing the specific electricity consumption of cultivation, harvesting, and extraction equipment is the single environmental impact of scaling. Table 3 describes the GHG emissions of pilot-scale and commercial-scale plants in addition to the emissions avoided as a result of scaling.

Table 3 – Reductions in Lifecycle Emissions from Reduced Electricity Requirements in 2192 BPD Facility

Scenario	Pilot Emissions from Electricity Use (gCO_2e/MJ_{HEFA-J})	Scaled Emissions from Electricity Use (gCO_2e/MJ_{HEFA-J})	Reduction in Lifecycle Emissions (gCO_2e/MJ_{HEFA-J})
Low	11.20	4.24	6.96
Baseline	16.00	6.06	9.94
High	79.20	30.01	49.19

Lifecycle emissions impacts from scaling range from 6.96 – 49.19 gCO_2e/MJ_{HEFA-J}, with a baseline impact of 9.94 gCO_2e/MJ_{HEFA-J}, or 32%. Figure 14 compares the lifecycle emissions of fuel produced in pilot and scaled facilities, including the variability of scaling impacts and variability described by Carter (2012).

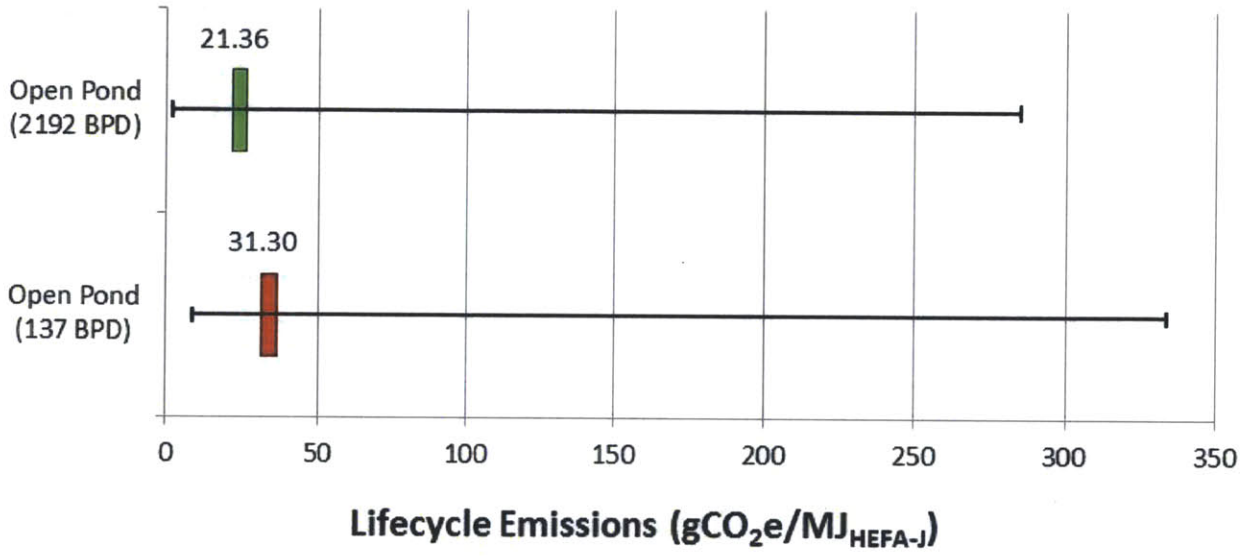

Figure 14 – Lifecycle GHG Emissions of Fuel Produced in 137 BPD and 2192 BPD Open Pond Systems

Assuming that the economic and environmental impacts of scaling are unaffected by the impacts of wastewater/aquaculture integration, it may be possible to combine integration and scaling techniques, resulting in the greatest overall impacts to fuel production cost and lifecycle GHG emissions. As integration with WWT facilities has been shown to result in greater overall impacts as compared to aquaculture integration, only WWT integration is considered in this portion of the analysis.

Adding the production cost impacts of scaling to the impacts of WWT integration serves to quantify the maximum production cost impact that may be achieved by open pond microalgae cultivation systems. Figure 15 illustrates the combined production cost impact in scaled open pond systems integrated with WWT facilities, and the individual contribution of each identified impact to the overall impact.

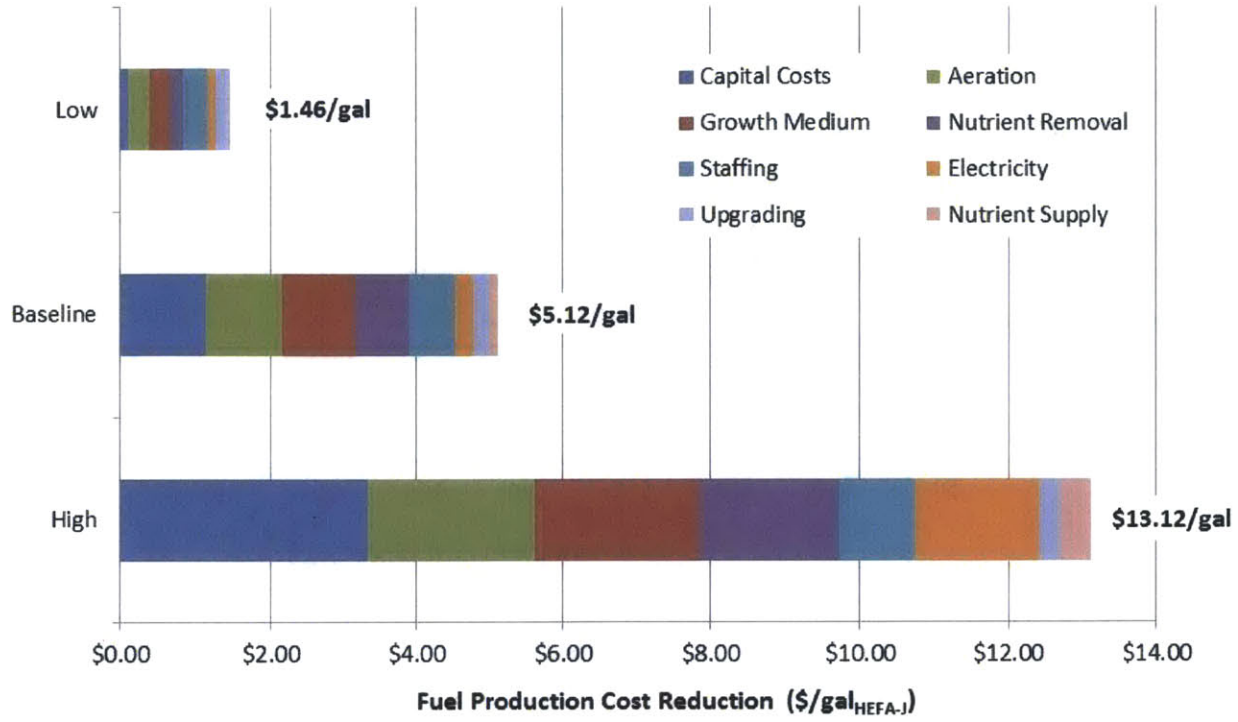

Figure 15 – Fuel Production Cost Reduction in a 2192 BPD Open Pond System with WWT Integration

Reductions in capital costs of installed equipment, aeration displacement, and reduced growth medium costs contribute over 50% of the total economic impacts in the baseline in high scenarios. In all scenarios, more significant economic impacts are seen from wastewater integration than from scaling.

Combined economic impacts range from \$1.46 - \$13.12/gal$_{HEFA-J}$, with an impact of \$5.12/gal$_{HEFA-J}$ or 52% in the baseline scenario. Figure 16 compares the resulting production cost of scaled/integrated and non-integrated pilot scale facilities, considering all aspects of variability. The resulting production cost of HEFA-J is \$4.74/gal for a scaled/integrated facility in the baseline scenario.

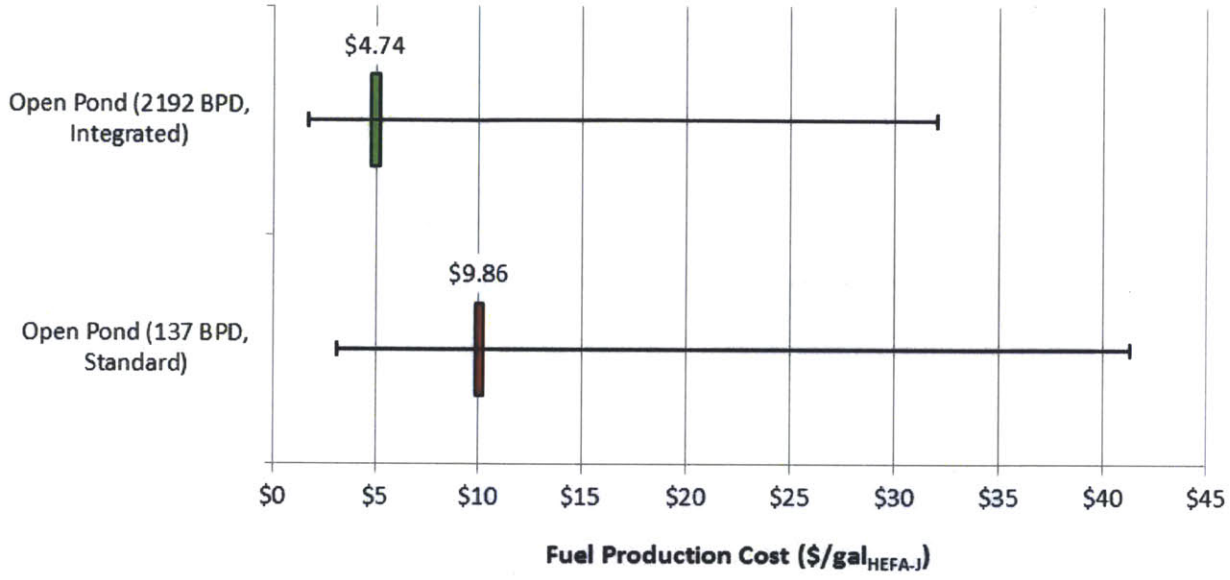

Figure 16 – Fuel Production Cost in Standard 137 BPD and WWT-Integrated 2192 BPD Open Pond Facilities

As with economic impacts, environmental impacts of scaling can be added to impacts from wastewater integration to quantify the maximum lifecycle GHG emissions impact that can be achieved by open pond systems. Figure 17 illustrates the total lifecycle GHG emissions avoided by a scaled/ integrated plant, and each impact's respective contribution to the overall impact.

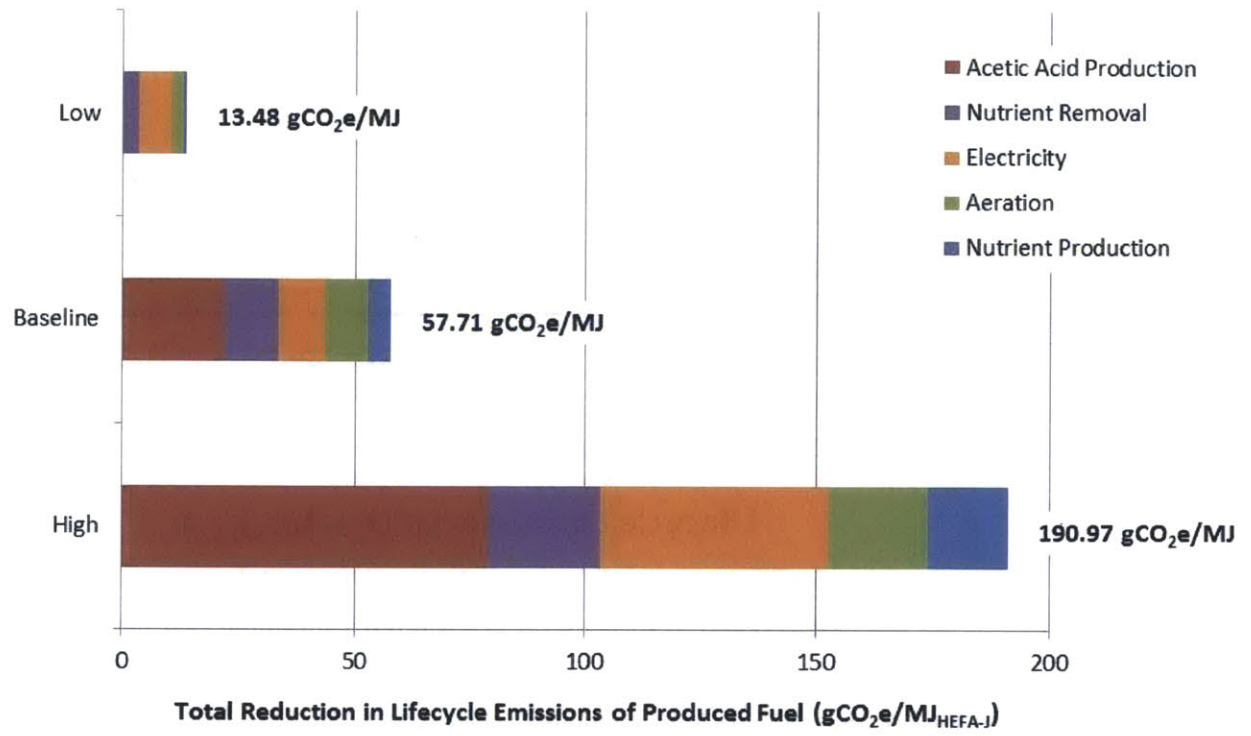

Figure 17 – Lifecycle GHG Emissions Reduction in a 2192 BPD Open Pond System with WWT Integration

Combined environmental impacts range from 13.48 – 190.97 gCO_2e/MJ_{HEFA-J}, with a baseline impact of 57.71 gCO_2e/MJ_{HEFA-J} or 184% in lifecycle emissions. Displacement of acetic acid production and nutrient removal contribute over 50% of the total impact in the baseline scenario.

Figure 18 compares the lifecycle emissions of fuel produced in integrated/scaled facilities to those of fuel produced in standard pilot facilities, and includes variability in impacts of integration and scale in addition to variability outlined in Carter (2012). By combining scaling and WWT integration impacts, lifecycle emissions of -26.41 gCO_2e/MJ_{HEFA-J} can be achieved in the baseline scenario for open pond systems.

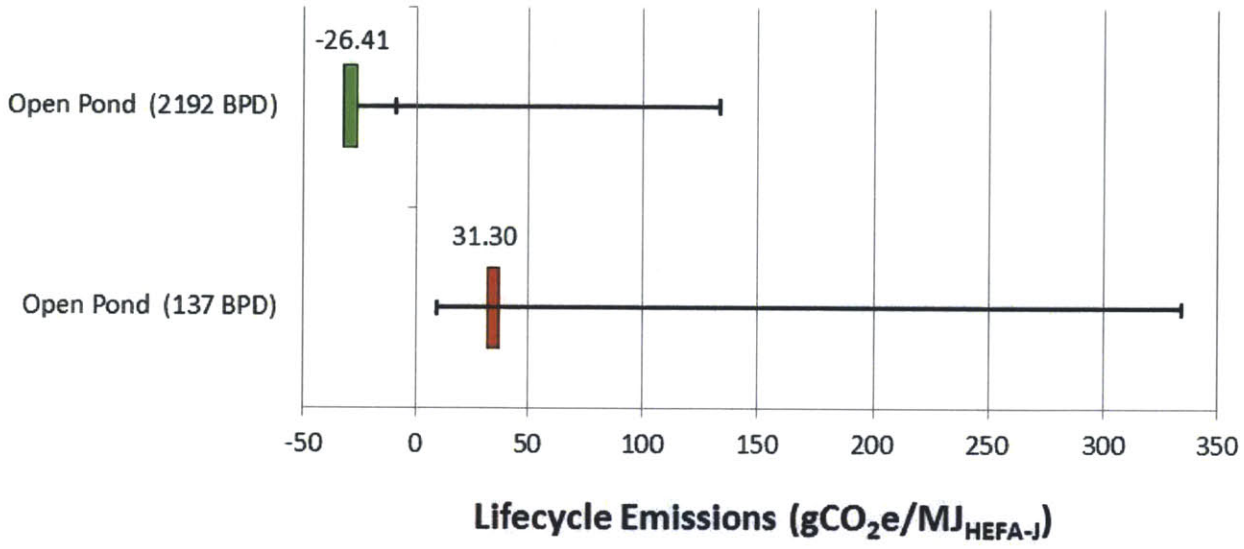

Figure 18 – Lifecycle Emissions of Fuel Produced in Standard 137 BPD and WWT-Integrated 2192 BPD Facilities

Table 4 summarizes the production cost and lifecycle GHG emissions of microalgae-derived HEFA-J in all systems and scenarios considered in this thesis.

Table 4 – Production Cost and Lifecycle GHG Emissions of Integration/Scaling Combinations

Scenario	System	Standard (Carter 2012)	Integrated (Wastewater)	Integrated (Aquaculture)	Scaled	Scaled + Wastewater Integration
Baseline	Open Raceway Pond	\$9.86/gal 31.3 gCO_2e/MJ	\$6.98/gal -16.47 gCO_2e/MJ	\$8.83/gal 31.15 gCO_2e/MJ	\$7.62/gal 21.36 gCO_2e/MJ	\$4.74/gal -26.41 gCO_2e/MJ
	Horizontal Tubular PBR	\$272.16/gal 202.00 gCO_2e/MJ	\$272.00/gal 187.44 gCO_2e/MJ	\$272.10/gal 201.99 gCO_2e/MJ	---	---
	Vertical Tubular PBR	\$614.88/gal 231.00 gCO_2e/MJ	\$614.82/gal 217.95 gCO_2e/MJ	\$614.86/gal 231.00 gCO_2e/MJ	---	---
	Flat Panel PBR	\$42.84/gal 54.00 gCO_2e/MJ	\$42.73/gal 40.10 gCO_2e/MJ	\$42.80/gal 53.39 gCO_2e/MJ	---	---
Low	Open Raceway Pond	\$2.30/gal 8.90 gCO_2e/MJ	\$1.77/gal -39.17 gCO_2e/MJ	\$2.03/gal 8.89 gCO_2e/MJ	\$1.59/gal 1.94 gCO_2e/MJ	\$0.84/gal -4.58 gCO_2e/MJ
	Horizontal Tubular PBR	\$79.38/gal 100.29 gCO_2e/MJ	\$79.30/gal 86.90 gCO_2e/MJ	\$79.36/gal 100.29 gCO_2e/MJ	---	---
	Vertical Tubular PBR	\$173.88/gal 101.26 gCO_2e/MJ	\$173.85/gal 89.52 gCO_2e/MJ	\$173.86/gal 101.26 gCO_2e/MJ	---	---
	Flat Panel PBR	\$16.38/gal 29.00 gCO_2e/MJ	\$16.32/gal 15.48 gCO_2e/MJ	\$16.36/gal 29.00 gCO_2e/MJ	---	---
High	Open Raceway Pond	\$40.10/gal 313.30 gCO_2e/MJ	\$33.49/gal 252.76 gCO_2e/MJ	\$38.18/gal 312.11 gCO_2e/MJ	\$33.81/gal 264.11 gCO_2e/MJ	\$26.98/gal 122.33 gCO_2e/MJ
	Horizontal Tubular PBR	\$1486.80/gal 637.00 gCO_2e/MJ	\$1486.44/gal 622.33 gCO_2e/MJ	\$1486.48/gal 636.04 gCO_2e/MJ	---	---
	Vertical Tubular PBR	\$1814.40/gal 646.00 gCO_2e/MJ	\$1814.04/gal 631.47 gCO_2e/MJ	\$1814.22/gal 645.04 gCO_2e/MJ	---	---
	Flat Panel PBR	\$104.58/gal 303.00 gCO_2e/MJ	\$104.44/gal 289.74 gCO_2e/MJ	\$104.48/gal 302.98 gCO_2e/MJ	---	---

3.4 – Global Bioenergy Potential

Values for annual areal energy yield of finished fuel throughout the world may be used to help identify areas most suitable for microalgae cultivation and fuel production. The calculation of these values are an integral part of determining the global bioenergy potential of microalgae. Figure 19 describes the results for the baseline scenario in units of GJ_{OIL}/ha/yr.

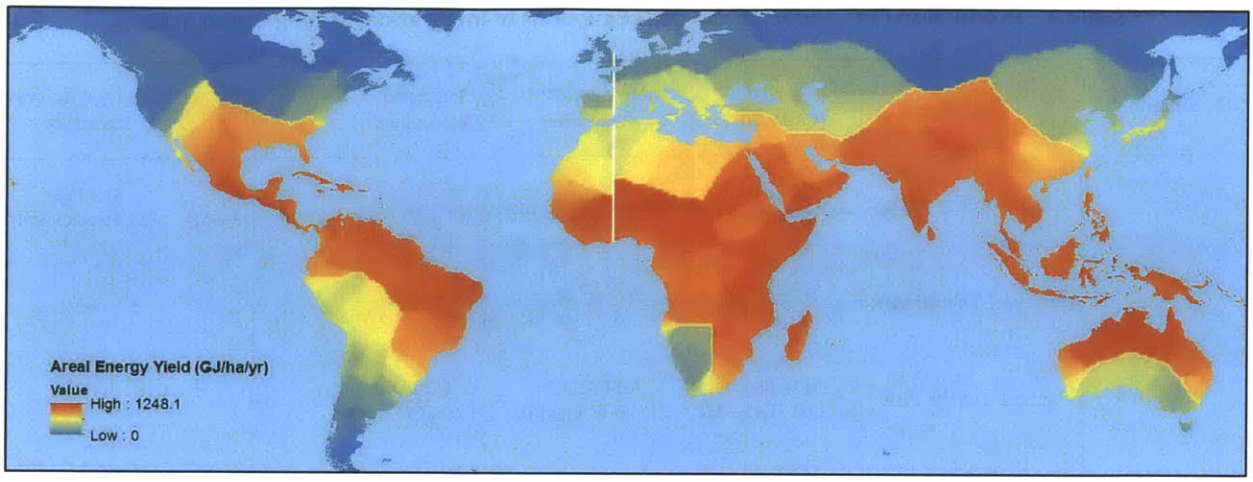

Figure 19 – Global Annual Areal Energy Yield of Oil in Baseline Scenario

Results indicate that optimal environmental characteristics for the cultivation of microalgae exist around the Gulf of Mexico, central Africa, India, Micronesia, and northern Australia, with a maximum areal energy yield of 1248.1 GJ_{OIL}/ha/yr or nearly 37,500 L_{HEFA-J}/ha/yr. In the low-constraint scenario, a maximum of 3448.6 GJ_{OIL}/ha/yr was calculated. The high-constraint scenario estimated a maximum of 661.7 GJ_{OIL}/ha/yr.

Imposing the geographical constraints described in Section 2.3 allows for the calculation of annual energy yield of finished fuel for each cell in units of GJ_{OIL}/yr. Figure 20 shows these results for the baseline scenario. Geographical constraints include water/CO_2 transportation constraints in addition to land slope and availability. However, CO_2 availability is not considered.

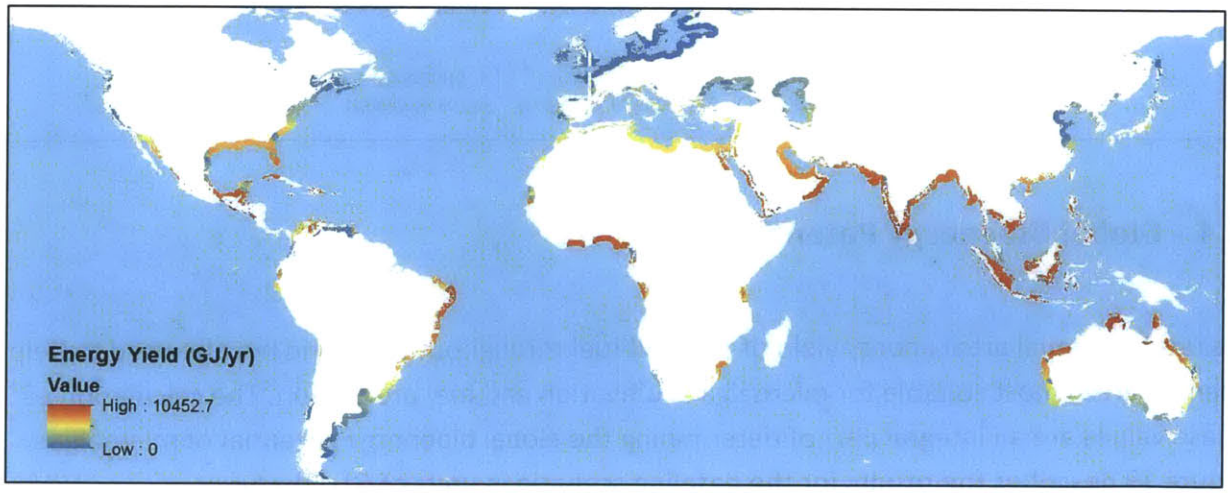

Figure 20 – Annual Energy Yield of Oil Constrained by Water/CO_2 Transportation and Land Slope/Availability

These results show that areas near the Gulf of Mexico, the Persian Gulf, southern India and Micronesia will produce the greatest annual quantity of energy from microalgae cultivation, but do not consider CO_2 availability constraints.

CO_2 saturation coefficients were calculated based on the mass of CO_2 required by and available to each cell. Figure 21 illustrates the CO_2 saturation coefficients calculated throughout the world for the baseline scenario.

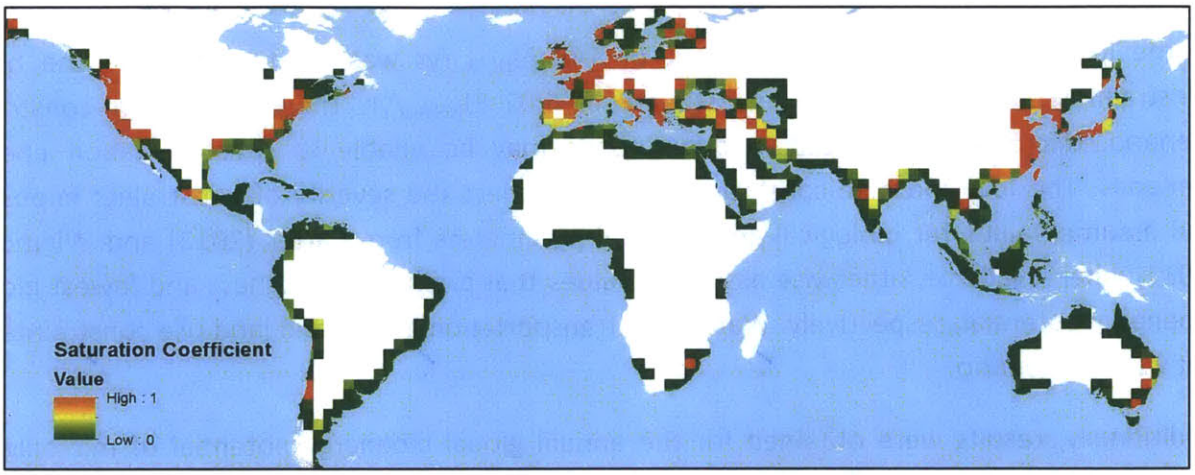

Figure 21 – CO_2 Saturation Coefficients in Baseline Scenario

Finally, Figure 22 illustrates the fully-constrained global bioenergy potential of microalgae-derived HEFA-J, separated by continent.

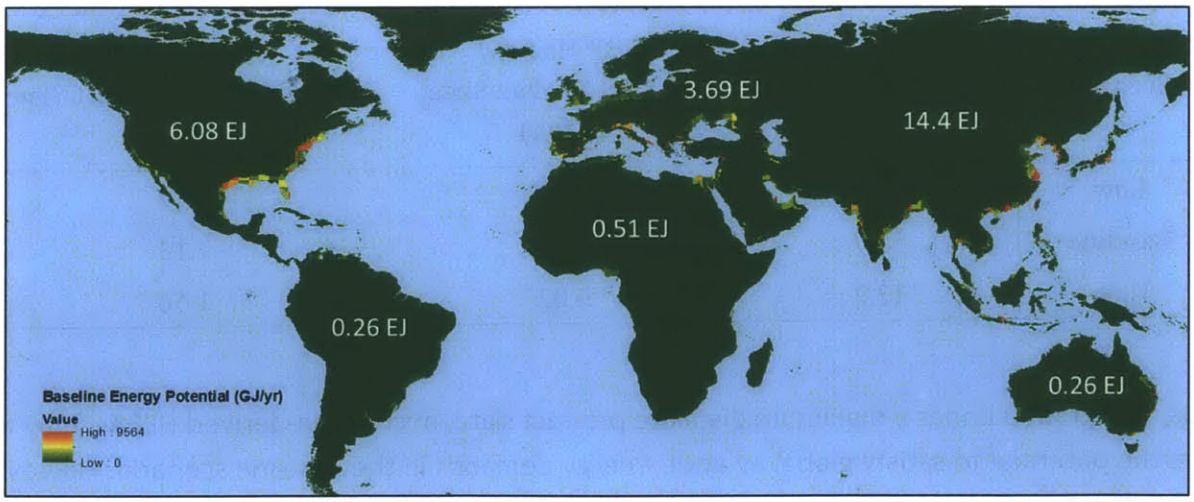

Figure 22 – Baseline Fully-Constrained Annual Finished Fuel Energy Yields and Regional Energy Potentials

In the baseline scenario, a summation of regional energy potentials of HEFA-J results in a global bioenergy potential of 27.5 EJ_{HEFA-J}/yr, or roughly 3 times the energy requirements of the aviation industry. It should be noted that the sum of regional energy potentials in Figure 22 is less than the global result of 27.5 EJ_{HEFA-J}/yr, as approximately 2.32 EJ_{HEFA-J}/yr is produced by island areas unassociated with a continent. Asia and North America have shown the greatest bioenergy potential from microalgae in the baseline scenario, at 14.4 EJ_{HEFA-J}/yr and 6.08 EJ_{HEFA-J}/yr, respectively. This is due in part to the favorable climatic conditions in these areas, and in part because of high CO_2 availability.

In the low-constraint scenario, a result of 148 EJ_{HEFA-J}/yr was estimated, while the high-constraint scenario resulted in an estimate of 6.02 EJ_{HEFA-J}/yr. Thus, in the high-constraint scenario, microalgae cultivated in open ponds may be unable to satisfy aviation energy demands. The low and high-constraint scenarios reflect the severity of constraints imposed, and assume values for biological and physical parameters from Carter (2012) and Wigmosta (2011) when available, otherwise assuming values that produce the highest and lowest global bioenergy potential, respectively. Water/CO_2 transportation, slope, and land use constraints do not vary by scenario.

Additionally, results were obtained for the annual global bioenergy potential of microalgae-derived HEFA-J when considering a maximum distillate product slate for the upgrading process, in which HEFA-J has a share of 12.8% (Carter, 2012). Table 5 summarizes the global bioenergy potential estimates for microalgae oil and HEFA-J for maximum jet/distillate product slates.

Table 5 – Global Bioenergy Potential Estimates for Microalgae Oil and HEFA-J for Maximum Jet/Distillate Product Slates

Scenario	GBP Microalgae Oil (EJ/yr)	GBP HEFA-J [Max Jet Product Slate] (EJ/yr)	GBP HEFA-J [Max Distillate Product Slate] (EJ/yr)
Low	300	148	38.4
Baseline	55.7	27.5	7.13
High	12.2	6.02	1.56

Thus, if upgraded under a maximum distillate product slate, microalgae-derived HEFA-J may not have the potential to satisfy global aviation energy demands in the baseline scenario. However, in the low-constraint scenario, available energy from HEFA-J still exceeds aviation energy demands by a factor of 4.3.

4 - Conclusions

This thesis quantifies the economic and environmental impacts that can be attained in the production of microalgae-derived HEFA jet fuel by integrating with wastewater/aquaculture facilities and scaling of production from pilot to commercial scale. Additionally, the annual global bioenergy potential of microalgae was assessed in order to determine the efficacy of microalgae as part of a diverse portfolio of energy feedstocks designed to produce sustainable fuels meeting a portion of global energy requirements at reduced levels of greenhouse gas emissions.

4.1 - Wastewater and Aquaculture Integration

Integration with wastewater treatment facilities has shown the potential to reduce the production cost of HEFA-J in microalgae facilities by $\$2.88/gal_{HEFA-J}$ in the baseline scenario for open pond systems, cutting production cost by nearly 30%. At a resulting production price of $\$6.98/gal_{HEFA-J}$, microalgae-derived jet fuel can be produced at 2.4 times the cost of conventional jet fuel via WWT-integrated open pond systems at pilot scale in the baseline scenario. With lifecycle greenhouse gas emissions being reduced to negative values through wastewater integration, integrated microalgae facilities may be able to displace a greater quantity of greenhouse gases than is emitted in the production of fuel.

Economic and environmental impacts resulting from WWT integration are driven heavily by the microalgae facility's ability to displace aeration and nutrient removal processes normally carried out by the WWT facility. As such, integration with WWT facilities that do not subject wastewater streams to these processes will not yield results of the magnitude estimated in this study. Additionally, integration with low-capacity WWT facilities may result in impacts lower than those described herein. However, it may be possible to integrate with a network of smaller WWT facilities in order to achieve maximum impacts.

Integration with aquaculture facilities also demonstrated economic benefits, but results were inferior to wastewater integration. A reduction in fuel production cost of $\$1.03/gal_{HEFA-J}$ was shown in the baseline scenario. However, environmental impacts were negligible at a reduction of < 0.5% lifecycle greenhouse gas emissions in all systems/scenarios. This may be attributed primarily to the lack of nutrient removal and aeration processes available for displacement in aquaculture facilities, and additionally to the low nutrient concentration of aquaculture effluent streams.

Integration techniques have been shown to be most effective in open pond systems, due to high water input requirements and the capacity to displace aeration and nutrient removal processes. Combined with initially lower production cost and greenhouse gas emission values as compared to photobioreactors (Carter, 2012), open ponds may have the greatest potential for production of sustainable jet fuel with low lifecycle greenhouse gas emissions.

The wide range of estimates for economic and environmental impacts from integration are due primarily to highly variable input requirements in addition to the varying costs and emissions of required inputs. The baseline scenario estimates are considered the most realistic, and are based on the work of Carter (2012). It should be reiterated that the high-scenario economic and environmental impact estimates may not be achievable in all systems. These estimates are the result of displacing inputs required in the high scenario, which are often more than twice the amount required in the baseline scenario (Carter, 2012).

4.2 - Scaling

Scaling of microalgae-derived jet fuel production in open pond systems has also been demonstrated to reduce the production cost of HEFA-J at a reduction of $\$2.24/gal_{HEFA\text{-}J}$ or 23%, making HEFA-J produced in commercial scale non-integrated facilities 2.6 times more expensive than conventional jet fuel, at $\$7.62/gal_{HEFA\text{-}J}$. Additionally, lifecycle GHG emissions are reduced to 21.36 $gCO_2e/MJ_{HEFA\text{-}J}$ as a result of scaling, making HEFA-J produced in scaled facilities 31.8% less GHG-intensive than HEFA-J produced in pilot facilities, and 75.6% less GHG-intensive than conventional jet fuel.

Scaling of cultivation, harvesting, and extraction equipment resulted in the greatest economic impact in the baseline scenario, even though open pond systems have relatively low capital costs (Carter, 2012). Systems with higher capital costs may be impacted more significantly through scaling.

Combining scaling and WWT-integration techniques in open pond systems results in maximum economic and environmental impacts, reducing fuel production cost and lifecycle emissions by $\$5.12/gal_{HEFA\text{-}J}$ and 57.71 $gCO_2e/MJ_{HEFA\text{-}J}$, respectively, in the baseline scenario. The resulting overall production cost is $\$4.74/gal_{HEFA\text{-}J}$, or 1.7 times that of conventional jet fuel. Lifecycle GHG emissions are reduced to -26.41 $gCO_2e/MJ_{HEFA\text{-}J}$, suggesting that an integrated and scaled microalgae facility displaces more GHG emissions than are generated through its production.

It should be noted that 100% of the microalgae cultivation facility's water input requirements are assumed to be satisfied by wastewater treatment facilities. This assumption may prove impractical in locating future fuel production facilities. In the baseline scenario, a scaled open

pond microalgae facility producing 2192 BPD of HEFA-J requires a water input of 92.2 million gallons per day.

Many metropolitan wastewater facilities have capacities exceeding this requirement, such as Deer Island Sewage Treatment Plant in Boston, MA with a capacity of 1.27 billion gallons per day and Stonecutters Island Sewage Treatment Works in Hong Kong with a capacity of 450 million gallons per day (ENR, 2014). However, treatment facilities of this scale typically exist in heavily urbanized areas, and may impose significant pumping costs and emissions in delivering a growth medium to an algae cultivation facility located externally.

4.3 - Global Bioenergy Potential

The analysis of the global bioenergy potential of microalgae imposed several constraints on the production of microalgae-derived jet fuel, resulting in estimates ranging from 12.2 – 300 EJ_{OIL}/yr with a baseline potential of 55.7 EJ_{OIL}/yr. Considering a maximum jet product slate, HEFA-J potential results range from 6.02 – 148 $EJ_{HEFA\text{-}J}/yr$, with a baseline potential of 27.5 $EJ_{HEFA\text{-}J}/yr$ or just over 3 times the global aviation energy demand. The greatest bioenergy production potential is seen in regions with expansive areas of marginal land, a tropical/semi-arid climate, and nearby high-capacity coal-fired and natural gas power plants.

The result of this study may serve as a tool for identifying areas throughout the world which are well-suited to the cultivation of microalgae. However, many other factors, such as cost of land and construction, should be taken into account when selecting a construction site for future microalgae cultivation facilities. These factors are not included in this study.

The resulting global bioenergy potential estimates demonstrate that microalgae have the potential to satisfy the global energy requirements of the aviation industry, and the baseline results of this analysis fall under the same order magnitude as two previously published works. One of these studies assessed the global energy potential of microalgae cultivated in open pond systems and reached an estimate of 90 EJ/yr (Florentinus et al., 2008). However, this study maintains a different set of assumptions, which allow for CO_2 supplementation with non-industrial sources and does not consider slope constraints.

The second study presents a range of global bioenergy potentials for microalgae between 40 – 1100 EJ/yr (Lysen, 2000). Several variables are considered, including biological parameters as well as land and water availability, resulting in the wide range of values.

4.4 - Suggestions for Future Studies

The integration analysis provided in this thesis addresses only four microalgae cultivation systems, three of which receive relatively little benefit from integration. With respect to production cost, impacts were negligible in photobioreactors systems in part due to the high capital costs associated with construction, and in part due to the low water input requirements of the systems. Several other microalgae cultivation technologies exist, such as floating bag and hybrid photobioreactors, which may experience different impacts as a result of integration compared to the systems analyzed herein (Frost & Sullivan, 2010).

Additionally, a significant degree of difficulty may exist in identifying sites with the necessary conditions to cultivate microalgae in scaled open pond systems with WWT integration. A high-resolution GIS analysis could be carried out to identify areas with suitable growth and construction parameters in addition to close-proximity, high-capacity WWT facilities or networks of low-capacity facilities. Quantifying the energy capacity of each area with respect to growth parameters and available wastewater is recommended.

Finally, several parameters considered in this assessment of global bioenergy potential of microalgae are expected to change by 2050. Consideration of trends in land use change and the global electricity generation portfolio, among others, should be taken to produce estimates for the global energy potential of microalgae in 2050 and ensure that current investment in microalgae cultivation systems will remain a sustainable strategy for producing low cost renewable fuels with low lifecycle greenhouse gas emissions.

Appendix A

Table 6 – Growth Medium Requirements (Carter, 2012)

System \ Scenario	Low	Baseline	High
Open Pond	1,555,731	5,762,290	12,882,115
Horizontal PBR	161,663	314,468	679,871
Vertical PBR	55,364	110,728	686,515
Flat Panel PBR	128,445	225,885	265,748

Table 7 – Nutrient Concentration in WWT and Aquaculture Effluent Streams (Carey & Migliaccio, 2009; Cripps & Bergheim, 2000)

	Wastewater Treatment		Aquaculture	
Scenario	N Concentration (mg/L)	P Concentration (mg/L)	N Concentration (mg/L)	P Concentration (mg/L)
Low	20	4	0.50	0.05
Baseline	45	9	2.75	0.155
High	70	14	5.00	0.26

Table 8 – Nutrient Inputs Requirements, Costs, and Emissions from Production (Carter, 2012; Wang, 2001)

	Nitrogen			Phosphorus Pentoxide		
Scenario	Input Required ($g/kg_{BIOMASS}$)	Cost ($/kg)	Emissions from Production (gCO_2e/kg)	Input Required ($g/kg_{BIOMASS}$)	Cost ($/kg)	Emissions from Production (gCO_2e/kg)
Low	36	$0.42		4	$1.00	
Baseline	100	$0.46	3,517	12	$1.20	671.5
High	173	$0.51		21	$1.40	

Table 9 – WWT Nutrient Removal Types, Costs, Electricity Consumption, and Acetic Acid Consumption/Emissions (Linden, 2001; Jones, 2000)

Scenario	Nutrient Removal Type	Cost ($/million gallons)	Electricity Consumption (kWh/million gallons)	Acetic Acid Consumption (gal/million gallons)	Emissions from Acetic Acid Production (gCO_2e/kg)
Low	UCT/VIP	$694.40	2,514	1,300	0
Baseline	CNC	$738.08	2,360	1,400	490
High	OWASA	$829.76	2,206	1,600	700

Table 10 – Aquaculture Biofiltration Techniques and Original/Converted Costs (Crab et al., 2007)

Scenario	Biofiltration Technique	Cost (€/kg_{FISH}/yr)	Cost (\$/$kg_{NITROGEN}$/yr)
Low	Fluidized Sand	0.198	\$2.08
Baseline	Bead Filters	0.503	\$5.28
High	Trickling Gravity Filtration	1.036	\$10.87

Table 11 – Cost of Electricity (U.S. Energy Information Administration, 2014)

Scenario	Cost of Electricity (\$/kWh)
Low	\$0.08
Baseline	\$0.13
High	\$0.17

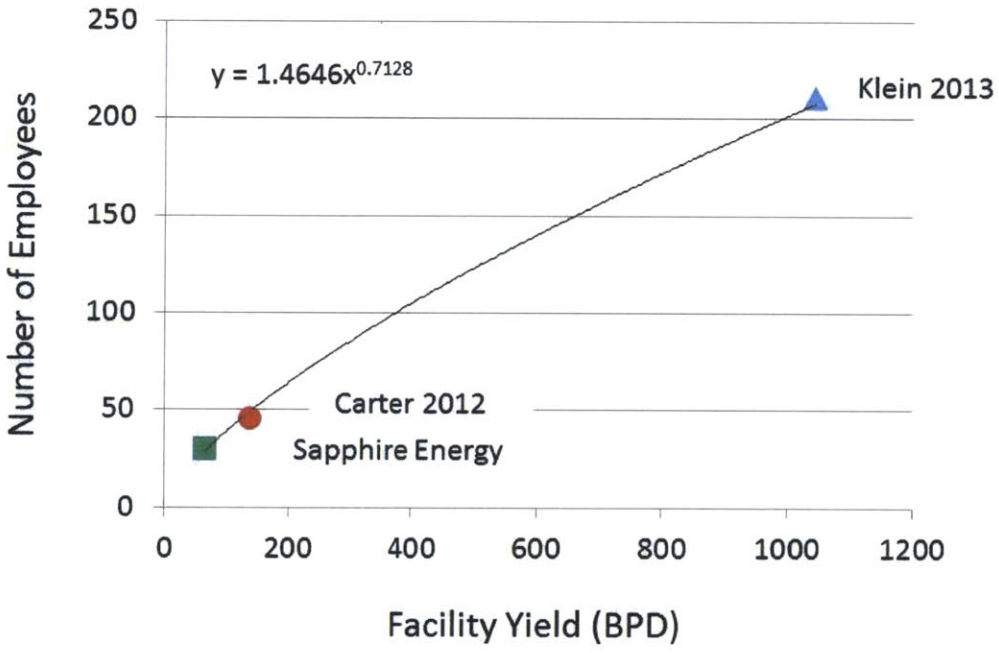

Figure 23 – Number of Employees versus Facility Yield (Sapphire Energy, Inc., 2014; Carter, 2012; Klein-Marcuschemer et al., 2013)

Table 12 – Employee Salaries and Required Number of Employees (Carter, 2012)

Scenario	Average Employee Salary	Number of Employees (Pilot)	Number of Employees (Scaled)
Low	$35,000	46	264
Baseline	$55,000	46	352
High	$72,000	46	440

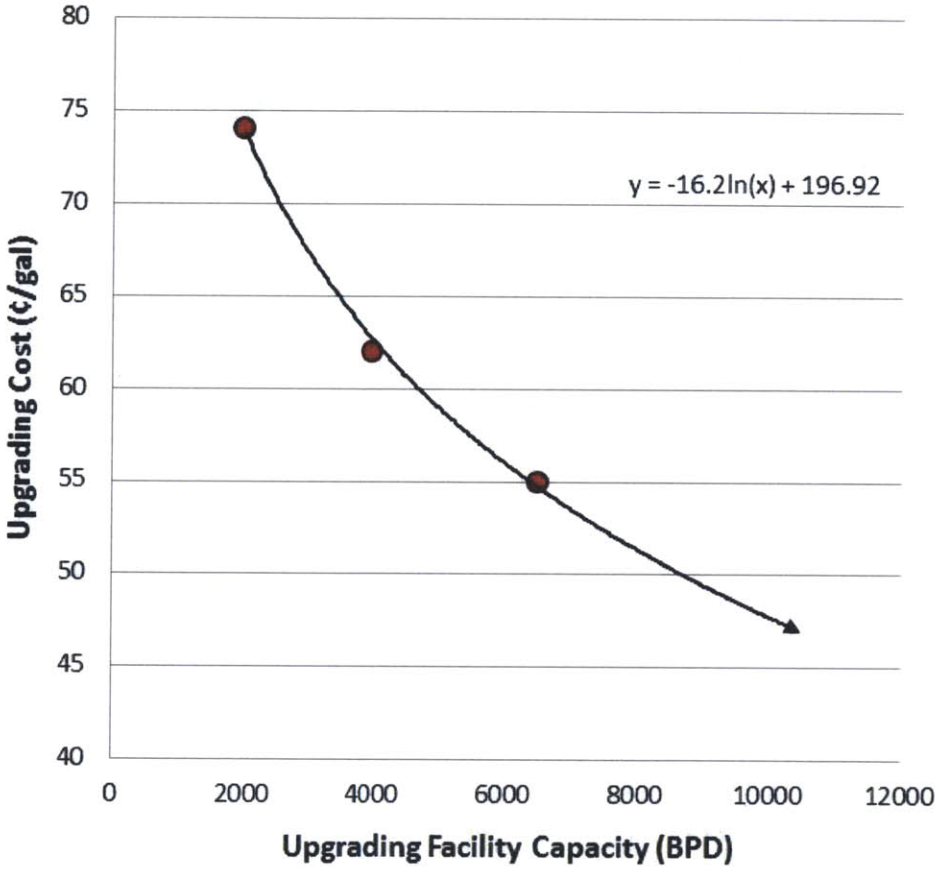

Figure 24 – Upgrading Cost versus Upgrading Facility Capacity (Pearlson, 2011)

Table 13 – Upgrading Facility Capacities and Upgrading Costs (Carter, 2012)

	Pilot Scale (137 BPD)		Commercial Scale (2192 BPD)	
Scenario	Upgrading Facility Capacity (BPD)	Upgrading Cost ($/gal$_{OIL}$)	Upgrading Facility Capacity (BPD)	Upgrading Cost ($/gal$_{OIL}$)
Low	2,000	$0.74	10,000	$0.48
Baseline	4,000	$0.62	16,000	$0.40
High	6,500	$0.55	19,500	$0.37

Table 14 – Specific Energy Inputs for Cultivation, Harvesting, and Extraction Processes (Carter, 2012)

Scenario	Cultivation Specific Energy (MJ/kg$_{BIOMASS}$)	Harvesting Specific Energy (MJ/kg$_{BIOMASS}$)	Extraction Specific Energy (MJ/kg$_{BIOMASS}$)	Total Specific Energy (MJ/kg$_{BIOMASS}$)
Low	0.8	0.4	0.2	1.4
Baseline	1.3	0.6	0.1	2.0
High	6.3	3.6	0.0	9.9

Table 15 – Cultivation, Harvesting, and Extraction Components with Closest-Matching Components

Component	Closest Matching Component	Notes
Open Ponds	Storage Tanks	Open pond construction physically similar to open-top storage tank construction
CO2 Feed System	Storage Tanks	CO2 feed system designed similar to pressurized storage tank
Water/Nutrient/Waste System	Pumps	Pumps are primary component of water/nutrient/waste system
Paddle Wheels	Motors	Paddle wheels driven by simple electric motor
Clarifiers	Clarifiers	-
Anaerobic Digesters	Storage Tanks	Anaerobic digesters are simply large storage tanks
CHP Units	CHP Units	-
Settling Ponds	Settling Ponds	-
DAFs	Clarifiers	DAF purpose/construction physically similar to clarifier purpose/construction
Belt Filter Presses	Belt Filter Presses	-

Table 16 – Installed Capital Costs and Scaling Exponents of Cultivation, Harvesting, and Extraction Components (Carter, 2012; McKetta, 2002)

Component	Low Capital Cost ($/MJ$_{HEFA-J}$)	Baseline Capital Cost ($/MJ$_{HEFA-J}$)	High Capital Cost ($/MJ$_{HEFA-J}$)	Scaling Exponent
Open Ponds	$0.00027	$0.00187	$0.00861	0.52 - 0.65
CO2 Feed System	-	$0.00150	$0.00342	0.52 - 0.65
Water/Nutrient/Waste System	$0.00021	$0.00182	$0.00460	0.5 - 0.9
Paddle Wheels	$0.00026	$0.00160	$0.00374	0.43 - 0.64
Clarifiers	-	$0.00267	-	0.98
Anaerobic Digester	$0.00011	$0.00096	$0.00225	0.52 - 0.65
CHP Units*	$0.00070	$0.00439	$0.01144	0.24
Settling Ponds	$0.00080	-	-	1.13
DAFs	-	-	$0.02214	0.98
Belt Filter Presses	-	-	$0.00107	0.58

*Scaling exponent for CHP units obtained from the U.S. Department of Energy's National Energy Technology Laboratory (2013).

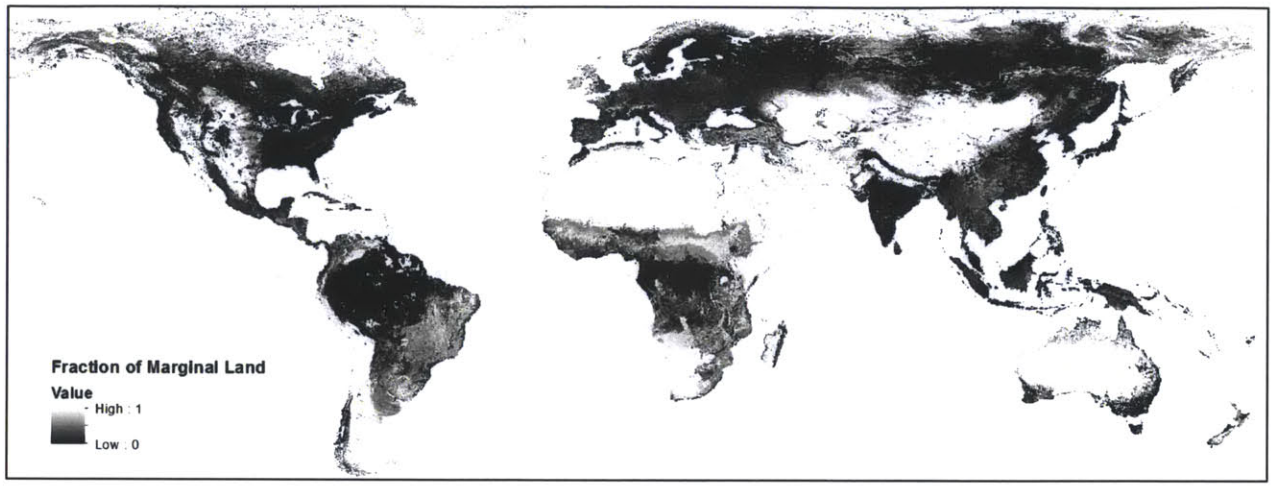

Figure 25 – Global Fractions of Marginal Land (Fischer et al., 2012)

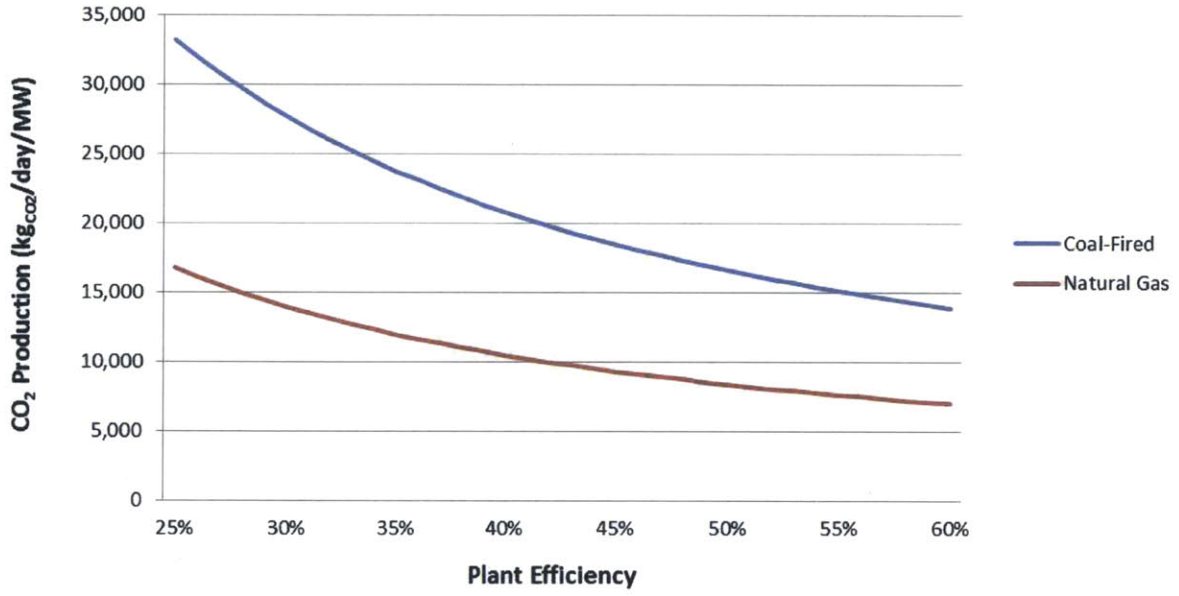

Figure 26 – CO_2 Production Rates per MW versus Power Plant Efficiency (Termuehlen & Emsperger, 2003)

Table 17 – Assumed Values for Geographically Constant Variables used in Global Bioenergy Assessment

Global Variable	Low Value	Baseline Value	High Value	Units	Reference
Microalgae Biomass LHV	32.80	32.80	32.80	$MJ/kg_{BIOMASS}$	Carter (2012)
Transmission Efficiency of Solar Radiation	0.90	0.90	0.90	-	Wigmosta et al. (2011)
Fraction of Photosynthetically Active Radiation	0.46	0.46	0.46	-	Wigmosta et al. (2011)
Photon Efficacy	1.86	2.38	2.90	µmol/J	Al-Shooshan (1997)
Extractable Lipid Fraction of Microalgae Biomass	0.60	0.25	0.15	-	Carter (2012)
Coal Power Plant Efficiency	0.25	0.33	0.45	-	World Coal Association (2014)
Coal Power Plant CO_2 Production	33,264	25,200	18,480	$kgCO_2/day/MW$	Termuehlen & Emsperger (2003)
Natural Gas Power Plant Efficiency	0.35	0.45	0.60	-	American Electric Power (2012)
Natural Gas Power Plant CO_2 Production	11,992	9,327	6,995	$kgCO_2/day/MW$	U.S. EPA (2014)
Microalgae CO_2 Inputs Requirements	2.43	2.05	1.93	$kgCO_2/kg_{BIOMASS}$	Carter (2012)
CO_2 Fixation Efficiency	0.90	0.90	0.90	-	Carter (2012)

[Page Intentionally Left Blank]

Appendix B

Literature has established that microalgae achieve optimum growth rates when cultivated in mediums with temperatures between 20°C - 30°C, reduced growth rates between 10°C - 20°C and 30°C - 35°C, and negligible growth or total culture loss at temperatures lower than 10°C or high than 35°C (Wigmosta et al., 2011). Table B1 describes the equations used to determine temperature correction factors with respect to temperature ranges of the growth medium.

Table 18 - Temperature Ranges of Growth Medium and Associated Temperature Correction Factor Equations (Wigmosta et al., 2011)

Temperature Range	Temperature Correction Factor
$T < 10°C$	0
$10°C \leq T < 20°C$	(T - 10) / 10
$20°C \leq T \leq 30°C$	1
$30°C < T \leq 35°C$	(35 - T) / 5
$T > 35°C$	0

Since seawater is used exclusively as the growth medium, it is assumed that the temperature of water at the surface of the nearest seawater body for any given inland location is equal to the temperature of that location's growth medium. Changes in growth medium temperature may occur during transportation, but are not considered in this study.

Thus, global datasets for monthly averages of sea surface temperature were obtained from the NOAA National Oceanographic Data Center and imported to ArcMap (part of the ArcGIS tool suite). A Euclidean allocation function was then used on all inland cells to determine the sea surface temperature of the nearest marine water source. Figure B1 illustrates the global temperature correction factors for the month of January, where blue indicates a coefficient of 0 and red indicates a coefficient of 1. It should be noted that these correction factors do not change in low or high scenarios, and that an error exists around 0° longitude due to an information gap in the NOAA data sets.

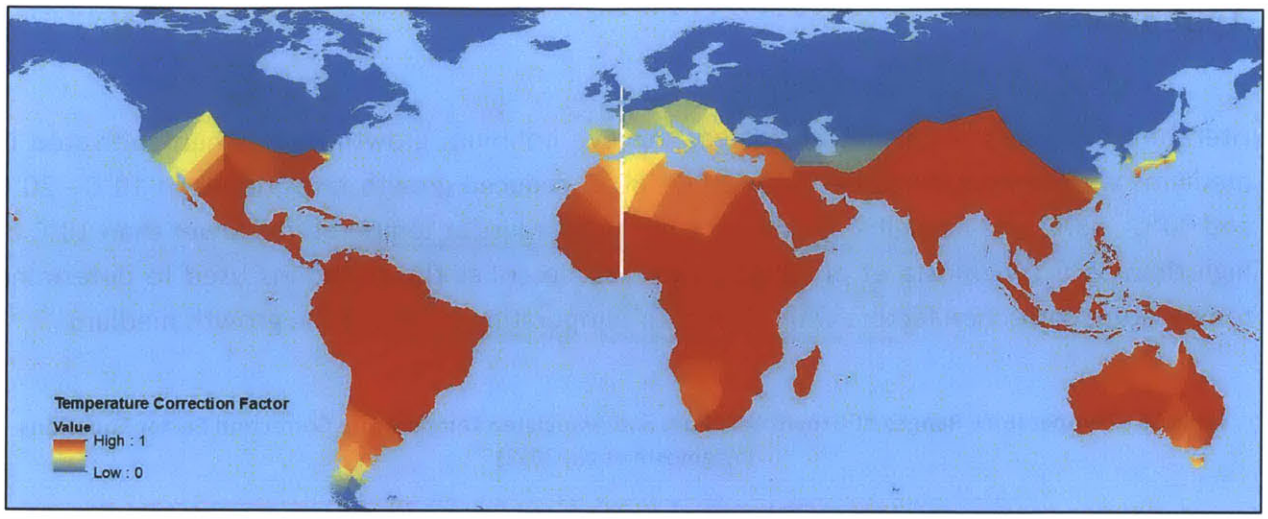

Figure 27 - Global Temperature Correction Factors for the Month of January

Areas near the equator provide growth mediums within the optimum temperature range for algae growth, and northern areas do not permit growth. This analysis was performed on all 12 monthly average sea surface temperature datasets for 2012.

Light utilization efficiency is described by Equation B1, adapted from Wigmosta et al. (2012),

$$\varepsilon_s = \frac{E_s}{S_0}\left(\ln\left(\frac{S_0}{E_s}\right) + 1\right) \qquad (B1)$$

where E_s is the full-spectrum radiation at the earth's surface, and S_0 is a value for light saturation, with units of μmol/s/m^2.

Before Equation B1 can be employed, E_s must be converted to units of μmol/s/m^2 (known as photon flux). Light saturation constants must also be calculated for each cell to be assessed in ArcMap.

Values for photon flux are calculated from monthly average global horizontal radiation datasets obtained from the NASA Atmospheric Science Data Center (given in J/m^2/s) by multiplying by photon efficacy values (see Table A12). Figure B2 illustrates the baseline photon flux values for the month of January, with units of μmol/s/m^2. Photon flux values were calculated for all 12 months in each scenario.

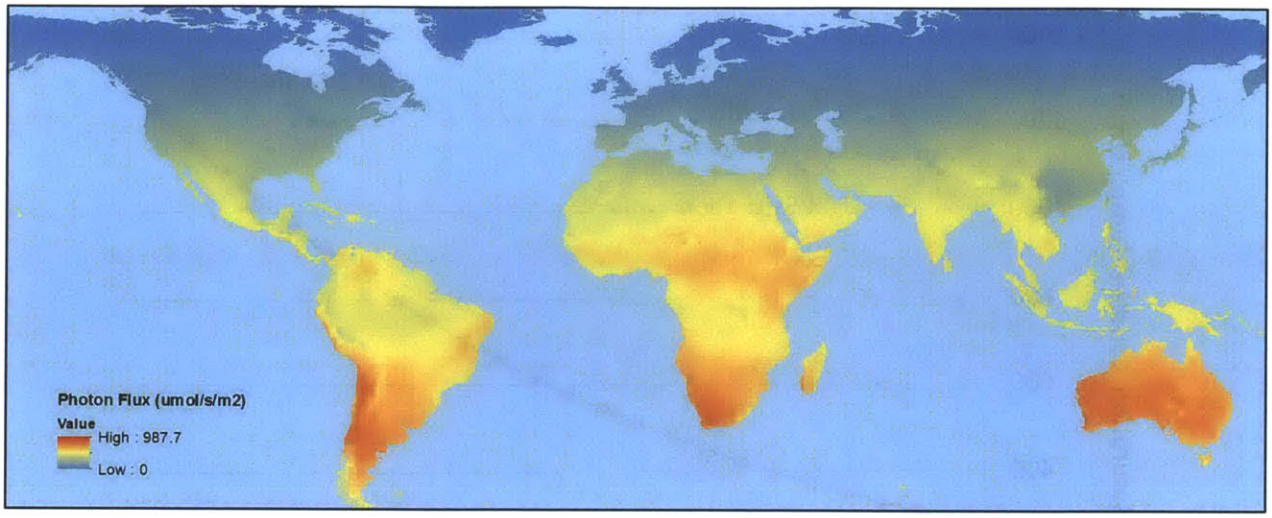

Figure 28 - Global Photon Flux Values for the Month of January in the Baseline Scenario

Light saturation constants quantify the amount of solar energy that microalgae require for fully-optimized photosynthesis, and have a complex relationship with growth medium temperature. As available existing literature is scarce, empirical data is used to describe this relationship. It should be noted that excessive solar energy can reduce the efficiency of photosynthesis, and "half-growth" light saturation constants quantify the solar intensity beyond the light saturation constant at which the growth reaches half of its optimum value.

Ahlgren (1987) provides data on several microalgae species cultivated in growth mediums of differing temperatures, which includes the corresponding light saturation and half-growth light saturation constants for each case. This data was plotted, and equations derived from fitted trend lines. Figure B3 illustrates these relationships and gives the corresponding equations, where x represents sea surface temperature.

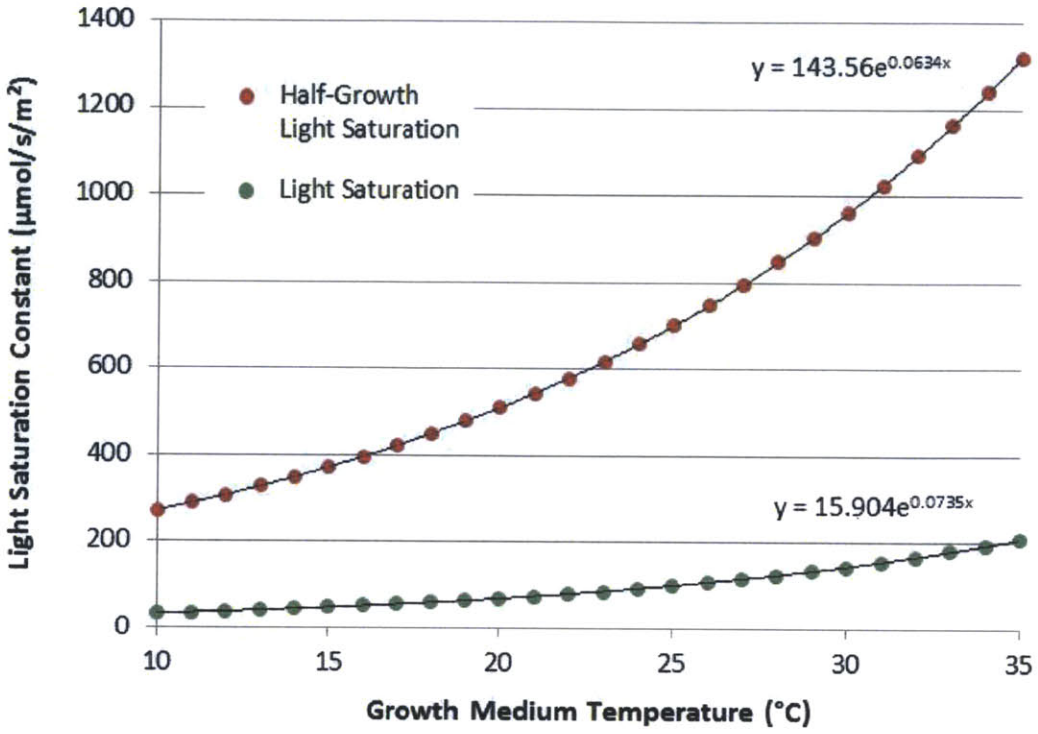

Figure 29 - Light Saturation and Half-Growth Light Saturation Constants of Microalgae at Varying Growth Medium Temperatures with Corresponding Equations (Ahlgren, 1987)

Calculations for light saturation constants follow Boolean logic where two distinct statements are used. If the incoming horizontal radiation is less than the light saturation constant, Equation B1 is used. However, if incoming horizontal radiation is greater than the light saturation constant, a modified version of Equation B1 is used in order to capture growth inhibition due to excessive solar energy. Equation B2 expresses this calculation,

$$\varepsilon_s = 1 - (E_s - S_0)(0.5/(S_{0.5} - S_0)) \qquad (B2)$$

where $S_{0.5}$ represents the half-growth light saturation constant, and assumes that inhibitions in photosynthesis efficiency follow a linear trend between full light saturation and half-growth light saturation.

By employing photon flux values with light saturation and half-growth light saturation values in Equations B1 and B2 as appropriate, global values for light utilization efficiency are produced. Figure B4 illustrates these results for January in the baseline scenario.

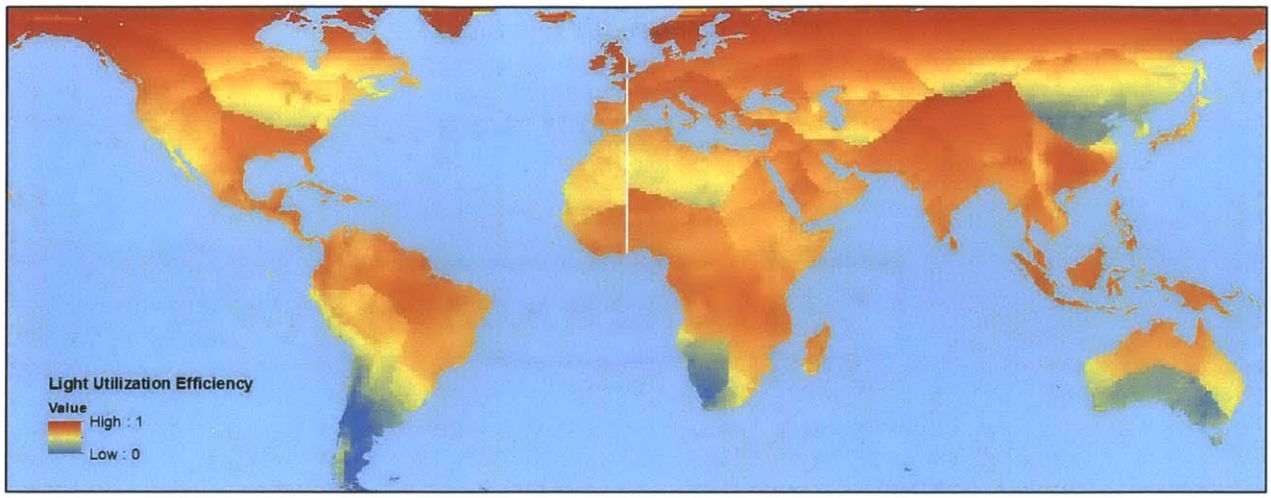

Figure 30 - Global Light Utilization Efficiency for January in the Baseline Scenario

The resulting values for temperature correction factors and light utilization efficiencies are used in Equation 3 to produce results for areal energy yield of microalgae biomass.

[Page Intentionally Left Blank]

Appendix C

An economic pumping analysis was carried out to determine the maximum pumping depth/distance acceptable for growth medium transportation. A threshold of $0.50/gal in growth medium pumping costs was selected as the economic maximum threshold. Water influent rates for open ponds in each scenario (Carter, 2012) were converted to gallons per minute and applied to Equation C1 in order to quantify pumping cost per gallon of HEFA-J,

$$C_{GAL} = \frac{(24)(0.746)\, Q\, h\, c}{(5754)(3960)\mu_p\, \mu_m} \qquad (C1)$$

where C_{GAL} represents pumping cost per gallon of HEFA-J, Q is equal to flow rate in gallons per minute, h is feet of head, c is the cost per kWh of electricity, μ_p is pump efficiency, and μ_m is motor efficiency (Engineering Toolbox, 2014).

Equation C1 is solved for h with C_{GAL} equal to $0.50. Q for an open pond in the baseline scenario is approximately 4,000 GPM (Carter, 2012). Cost of electricity is assumed to be the global average of $0.11/kWh (U.S. EIA, 2010), and the efficiencies of pumps and motors are assumed to be 0.8 (Carter, 2012).

Based on these parameters, a maximum pumping depth of 982 feet was calculated. As shallow saline aquifers (with a depth less than 500 meters) are scarce, with many dedicated to other uses (IGRAC, 2009), saline aquifers are not considered as potential growth medium sources.

The Hazen-Williams equation was employed to calculate head loss per hundred feet of horizontal pipe. Equation C2 illustrates this equation,

$$f = \frac{0.2083\left(\frac{100}{c}\right)^{1.852} q^{1.852}}{d_h^{4.8655}} \qquad (C2)$$

where f is head loss (in feet) per hundred feet of pipe, q is flow rate, c is a roughness constant held at 140 (Engineering Toolbox, 2014) and d_h is pipe diameter, which is assumed to be 24 inches.

Head loss was determined to be 0.101 ft per hundred feet of pipe or 0.00101 ft per foot of pipe. By dividing the maximum pumping head of 982 ft by this value, a maximum horizontal pumping distance of 100 miles was calculated. This distance constraint is assumed throughout the global bioenergy potential analysis, and is of similar magnitude to the value assumed by Florentinus et al. (2008), which assumes a maximum water transportation distance of 100 kilometers (62 miles).

References

Ahlgren, G. (1987, June). Temperature Functions in Biology and their Application to Algal Growth Constants. *Oikos, 49*(2), 177-190.

Al-Shooshan, A. A. (1997). Estimation of Photosynthetically Active Radiation under an Arid Climate. *Journal of Agricultural Engineering Research, 66*, 9-13.

American Electric Power. (2012, August). *Natural Gas Technology*. Retrieved March 2014, from AEP: http://www.aep.com/about/IssuesAndPositions/Generation/Technologies/NaturalGas.aspx

Atmospheric Science Data Center. (2005). *NASA Surface meteorology and Solar Energy: Global Data Sets.* NASA.

Benemann et al. (1982). *Microalgae as a source of liquid fuels.* Proceedings of the June 1982 SERI Biomass Program Principal Investigators' Review Meeting, Aquatic Species Program Reports.

Carey, R. O., & Migliaccio, K. W. (2009). Contribution of Wastewater Treatment Plant Effluents to Nutrient Dynamics in Aquatic Systems: A Review. *Environmental Management, 44*, 205-217.

Carter, N. A. (2012). *Environmental and Economic Assessment of Microalgae-derived Jet Fuel.* SM Thesis, Department of Aeronautics and Astronautics, Massachusetts Institute of Technology, Cambridge, MA.

Crab et al. (2007). Nitrogen removal techniques in aquaculture for sustainable production. *Aquaculture, 270*, 1-14.

Cripps, S. J., & Bergheim, A. (2000). Solids management and removal for intensive land-based aquaculture production systems. *Aquaculture Engineering, 22*, 33-56.

Davis et al. (2014). Integrated Evaluation of Cost, Emissions, and Resource Potential for Algal Biofuels at the National Scale. *Environmental Science & Technology*.

Eggers, R. (2013). *Crude Oil and Transportation Fuel Price Cases for the 2013 IEPR.* Fuels and Transportation Division, Transportation Energy Office. California Energy Commission.

Engineering Toolbox. (2014). *Hazen-Williams Coefficients*. Retrieved February 2014, from The Engineering Toolbox: http://www.engineeringtoolbox.com/hazen-williams-coefficients-d_798.html

Engineering Toolbox. (2014). *Water Pumping Costs*. Retrieved from http://www.engineeringtoolbox.com/water-pumping-costs-d_1527.html

ENR. (2014). *The 10 Largest Wastewater Treatment Plants*. Retrieved August 2013, from Engineering News Record:

http://enr.construction.com/infrastructure/water_dams/2012/extras/0328/slideshow.asp?slide=1

Fischer et al. (2012). *Global Agro-Ecological Zones (GAEZ v3. 0) – Model Documentation.* International Institute for Applied systems Analysis (IIASA), Austria and the Food and Agriculture Organization of the United Nations (FAO). Rome, Italy: Laxenburg.

Fischer, G., & Schrattenholzer, L. (2001). Global bioenergy potentials through 2050. *Biomass and Bioenergy, 20*, 151-159.

Florentinus et al. (2008). *Worldwide Potential of Aquatic Biomass.* Dutch Ministry of the Environment. Utrecht: Ecofys.

Freyberg, T. (2011, February). Algae Biofuel. *WaterWorld, 27*(2).

Frost & Sullivan. (2010, August 20). *Algasol Renewables*. Retrieved September 29, 2014, from Frost & Sullivan Recognizes Algasol Renewables for its Micro Algae Biomass Production System: http://www.algasolrenewables.com/Common/Documents/UserFiles/Algasol%20Renewables%20Award%20PR_FINAL.pdf

Global CCS Institute. (2012, October). CO2 Transportation Costs. *The Global Status of CCS*.

Hu et al. (2008). Microalgal triacylglycerols as feedstocks for biofuel production: perspectives and advances. *The Plant Journal, 54*, 621-639.

ICAO. (2010). *ICAO Environmental Report.* ICAO.

ICAO. (2013). *ICAO Environmental Report 2013.* Environment Branch of the International Civil Aviation Organization.

IGRAC. (2009). *Saline and brackish groundwater by genesis.* International Groundwater Resources Assessment Centre.

International Air Transportation Association. (2013). *Financial Forecast.* Industry Financial Forecast, IATA Economics.

IPCC. (1999). *Aviation and the Global Atmosphere.* Intergovernmental Panel on Climate Change.

Islam, M. S. (2005). Nitrogen and phosphorus budget in coastal and marine cage aquaculture and impacts of effluent loading on ecosystem: review and analysis towards model development. *Marine Pollution Bulletin, 50*, 48-61.

Jet Propulsion Laboratory. (2011). *ASTER Global Digital Elevation Map.* California Institute of Technology. Pasadena : NASA.

Jining, C., & Junying, C. (2004). Municipal Effluent Disposal Standards. *Point Sources of Pollution: Local Effects and Its Control, 1*.

Jones, J. H. (2000). The Cativa Process for the Manufacture of Acetic Acid. *Platinum Metals Review, 44*(3), 94-105.

Klein-Marcuschemer et al. (2013, February). Technoeconomic analysis of renewable aviation fuel from microalgae, Pongamia pinnata, and sugarcane. *Biofuels, Bioproducts & Biorefining, 7*, 416-428.

Linden, K. G. (2001). *Evaluation of Performance and Operational Costs for Three Biological Nutrient Removal Schemes at a Full-Scale Wastewater Treatment Plant.* Duke University, Department of Civil and Environmental Engineering, Durham, NC.

Lysen, E. H. (2000). *Global Restrictions of biomass availability for import to the Netherlands.* Utrecht: Novem.

McCollum, D., & Yang, C. (2009). Achieving deep reductions in US transport greenhouse gas emissions: Scenario analysis and policy implications. *Energy Policy, 37*, 5580-5596.

McKetta, J. (2002). *Encyclopedia of Chemical Processing and Design* (Vol. 43). M. Dekker.

Menetrez, M. Y. (2012). An Overview of Algae Biofuel Production and Potential Environmental Impact. *Environmental Science and Technology, 46*, 7073-7085.

Muhs et al. (2009). *A summary of opportunities, challenges, and research needs: algae biofuels & carbon recycling.* Utah State University.

National Energy Technology Laboratory. (2013). *Capital Cost Scaling Methodology.* U.S. Department of Energy.

NODC. (2012). *Pathfinder SST.* United States Department of Commerce, NOAA Satellite and Information Service.

Olguin, E. J. (2012). Dual purpose microalgae–bacteria-based systems that treat wastewater and produce biodiesel and chemical products within a Biorefinery. *Biotechnology Advances, 30*, 1031-1046.

Pearlson, M. N. (2011). *A Techno-Economic and Environmental Assessment of Hydroprocessed Renewable Distillate Fuels.* SM Thesis, Massachusetts Institute of Technology, Department of Aeronautics and Astronautics, Cambridge, MA.

Platts. (2014). *World Electric Power Plants Database.* McGraw Hill Financial.

Sapphire Energy, Inc. (2014, February). Retrieved August 2013, from Sapphire Energy: http://www.sapphireenergy.com/sapphire-renewable-energy

Stratton et al. (2010). *Life Cycle Greenhouse Gas Emissions from Alternative Jet Fuels.* Partnership for Air Transportation Noise and Emissions Reduction.

Termuehlen, H., & Emsperger, W. (2003). *Clean and Efficient Coal-Fired Power Plants.* ASME Press.

The World Bank Group. (2014). *The World Bank*. Retrieved January 16, 2014, from worldbank.org: http://water.worldbank.org/shw-resource-guide/infrastructure/menu-technical-options/wastewater-treatment

U.S. EIA. (2010). *Electricity Prices for Industry for Selected Countries.*

U.S. Energy Information Administration. (2014). *Electric Power Monthly.* U.S. Department of Energy, Washington, DC.

U.S. EPA. (2014). *Natural Gas*. Retrieved January 2014, from Clean Energy: http://www.epa.gov/cleanenergy/energy-and-you/affect/natural-gas.html

Wang, M. (2001). *Development and use of GREET 1.6 fuel-cycle model for transportation fuels and vehicle technologies.* Argonne National Laboratory, Chicago, IL.

Weyer et al. (2010). Theoretical Maximum Algal Oil Production. *Bioenergy Research, 3*, 204-213.

Wigmosta et al. (2011). National microalgae biofuel production potential and resource demand. *Water Resources Research, 47*, 1-13.

Woertz et al. (2009, November). Algae Grown on Dairy and Municipal Wastewater for Simultaneous Nutrient Removal and Lipid Production for Biofuel Feedstock. *Journal of Environmental Engineering, 135*, 1115-1122.

World Coal Association. (2014, March). *Improving Efficiencies*. Retrieved March 2014, from WorldCoal: http://www.worldcoal.org/coal-the-environment/coal-use-the-environment/improving-efficiencies/